

# Abstract

---

Gait analysis is presently a common and useful tool for both biomechanical research and clinical practice. A lot of studies have developed multi-segment foot models in order to characterize foot kinematics. However, very few studies deal with dynamic analysis and no validation has yet been done. The present study proposes a multi-segment foot model that allows assessment of movements and mechanical actions within the foot.

The instrumentation consists in a Motion Analysis<sup>®</sup> System with eight Eagle<sup>®</sup> cameras and two Bertec<sup>®</sup> forceplates. One RsScan<sup>®</sup> baropodometric plate is also used. Ten healthy people are involved in this study. For each subject, ten gait trials are collected combining kinematic, dynamic and baropodometric information. An original method of external actions distribution based on Coulomb's laws will be used for inverse dynamics computation.

The results are consistent with literature data and additional information (joint angles and joint moments) is available with the present study. Future works involving more subjects will provide the statistical analysis required to assess the detection of pathologic cases.





## Resumen

---

El análisis de la marcha es actualmente un medio común y útil tanto para la investigación en biomecánica como para la práctica clínica. Muchos estudios han desarrollado un modelo de pie con varios segmentos para caracterizar su cinemática. No obstante, pocos de ellos realizan un estudio dinámico y aún no se encuentran validados. En este trabajo se presenta un modelo de pie con varios segmentos que permite la evaluación de los movimientos y de las acciones mecánicas en el pie.

La instrumentación consiste en un sistema Motion Analysis<sup>®</sup> con ocho cámaras Eagle<sup>®</sup> y dos plataformas de fuerza Bertec<sup>®</sup>. Se utiliza también una plataforma baropodométrica RsScan<sup>®</sup> para medidas de presión plantar. El estudio se ha realizado sobre diez personas sanas. Para cada una de ellas, se han realizado diez ensayos de marcha combinando mediciones de tipo cinemático, dinámico y baropodométrico. Se utiliza un método original de repartición de acciones externas basado en las leyes de Coulomb para el análisis dinámico inverso.

Los resultados son coherentes con la literatura y además se han encontrado nuevos resultados de ángulos y momentos articulares entre los segmentos del pie. Futuros trabajos con más personas permitirían realizar el análisis estadístico necesario para el diagnóstico de casos patológicos.





# Index

<b>Abstract .....</b>	<b>1</b>
<b>Resumen .....</b>	<b>3</b>
<b>Index .....</b>	<b>5</b>
<b>Illustration Index.....</b>	<b>7</b>
<b>Table Index.....</b>	<b>9</b>
<b>Glossary .....</b>	<b>11</b>
Definitions.....	11
Acronyms.....	11
<b>Introduction.....</b>	<b>13</b>
<b>1. Anatomical and Biomechanical Notions.....</b>	<b>15</b>
1.1 Body Planes .....	15
1.2 Lower Limb Functional Anatomy .....	16
1.3 Gait Cycle .....	17
1.4 Foot Description .....	18
1.4.1 Foot Bones .....	18
1.4.2 Foot Movements.....	19
<b>2. State of the art – Problematic.....</b>	<b>23</b>
2.1 State of the Art .....	23
2.1.1 Existing Models .....	24
2.1.2 Source of Errors .....	27
2.1.3 Correction Methods .....	27
2.1.4 Normalized Moments .....	30
2.1.5 Synthesis Table .....	31
2.2 Problematic.....	35
<b>3. Materials and Protocol.....</b>	<b>37</b>
3.1 Materials .....	37
3.1.1 Motion Analysis® System .....	38
3.1.2 Force Plates .....	39
3.1.3 Plantar Pressure Plate .....	40
3.1.4 Landmarks Definition.....	41



3.2 Protocol.....	41
3.2.1 Preparation and Subject Trials .....	41
3.2.2 Data Tracking .....	44
<b>4. Methodology .....</b>	<b>47</b>
4.1 Kinematic Analysis.....	47
4.1.1 Segments Definition and Coordinate Systems.....	47
4.1.2 Angular Rotation Calculation .....	49
4.2 Dynamic Analysis .....	52
4.2.1 Inverse Dynamics .....	52
4.2.2 External Actions Repartition .....	54
4.2.3 Body Segments Inertial Parameters.....	59
<b>5. Results and discussion .....</b>	<b>63</b>
5.1 Kinematics .....	63
5.1.1 Litterature Comparison .....	63
5.1.2 Present Study Contribution.....	65
5.2 Measurement Repeatability.....	65
5.3 External Actions Distribution.....	66
5.4 Dynamics .....	67
5.4.1 Litterature Comparison .....	67
5.4.2 Present Study Contribution.....	69
<b>Conclusions .....</b>	<b>71</b>
<b>Acknowledgements .....</b>	<b>73</b>
<b>Bibliography .....</b>	<b>75</b>
<b>Appendices .....</b>	<b>79</b>
A.1 Economical Cost .....	79
A.2 Environmental and Social Impact.....	81
A.3 SCS Definition .....	82
A. 4 BSIP .....	83
A.5 Euler Angle Sequence Matrix.....	84
A.6 Check List for Trials.....	85
A.7 Accepted Abstract .....	89



# Illustration Index

Figure 1.1 – Body Planes.....	15
Figure 1.2 – Lower Limbs.....	16
Figure 1.3 – A Human Gait Cycle.....	17
Figure 1.4 – Foot Bones.....	19
Figure 1.5 – Foot Axes.....	19
Figure 2.1 – Oxford Foot Model.....	24
Figure 2.2 – Leardini Foot Model.....	25
Figure 2.3 – Jenkyn Foot Model.....	25
Figure 2.4 – Heidelberg Foot Model.....	26
Figure 2.5 – Mac Williams Foot Model.....	26
Figure 2.6 – Invasive Markers.....	28
Figure 2.7 – Plates Mounted Markers.....	29
Figure 2.8 – Methods Compared.....	29
Figure 3.1 – Laboratory Disposition.....	37
Figure 3.2 – Markers.....	38
Figure 3.3 – Calibration Square.....	39
Figure 3.4 – Calibration Wand.....	39
Figure 3.5 – Data Available.....	40
Figure 3.6 – Landmarks.....	41
Figure 3.7 – Markers Position.....	43
Figure 3.8 – RsScan® Pressure Map.....	45
Figure 4.1 – Segments Location.....	46
Figure 4.2 – Leg and Foot SCS.....	49
Figure 4.3 – Euler Axes.....	50
Figure 4.4 – Knee Euler Axes.....	51
Figure 4.5 – Inverse Dynamics Approach.....	53
Figure 4.6 – Forceplate Data Available.....	54
Figure 4.7 – Data Necessary.....	55
Figure 4.8 – Pressure Map.....	55
Figure 4.9 – Masks Allocation.....	56
Figure 4.10 – Sections Corresponding to the Activated Masks.....	56
Figure 4.11 – Masks Ratio.....	57
Figure 4.12 – CoP for Each Segment.....	57
Figure 4.13 – GRF Distribution during SP.....	58
Figure 4.14 – Toe and FF in Contact with the Floor.....	59
Figure 4.15 – Foot SCS.....	59
Figure 5.1 – Kinematic Comparison.....	63
Figure 5.2 – Additional Angles.....	65
Figure 5.3 – Ground Reaction Force.....	65
Figure 5.4 – External Actions Distribution.....	66
Figure 5.5 – Dynamic Comparison.....	67
Figure 5.6 – Additional Moments.....	69







# Table Index

---

Table 1.1 – Foot Movements.....	21
Table 2.1 – Foot Models Synthesis Table.....	31
Table 4.1 – Segments Definition.....	48
Table 4.2 – Scaling Factors.....	60
Table 4.3 – Subject 1 BSIP.....	61
Table A.1.1 – Depreciation Costs.....	79
Table A.1.2 – Used Hours.....	79
Table A.1.3 – Global Cost.....	80
Table A.5.1 – BSIP Coefficients for Men.....	83
Table A.5.2 – BSIP Coefficients for Women.....	83





# Glossary

---

## Definitions

**Center of Pressure:** The point on the surface of the forceplate through which the ground reaction force acts. It corresponds to the projection of the subject's center of gravity on the forceplate surface when the subject is motionless. (Bertec® manual definition)

**Distal:** Segment edge that is more distant to the center of the body.

**Proximal:** Segment edge that is closer to the center of the body.

**Spherical Joint:** Mobile Joint with spherical surfaces, one is convex and the other concave. This allows three degrees of freedom between the linked parts.

**Stance Phase:** Gait cycle phase during which the foot is in contact with the floor.

**Swing Phase:** Gait cycle phase during which the foot is not in contact with the floor while the other one is.

## Acronyms

**BSIP:** Body Segment Inertial Parameters

**CoM:** Centre of Mass

**CoP:** Centre of Pressure

**DoF:** Degree of Freedom

**FF:** ForeFoot

**FPD:** Fundamental Principle of Dynamics

**HF:** HindFoot

**HX:** Hallux

**ISB:** International Society of Biomechanics

**JCS:** Joint Coordinate System

**LL:** Laboratory Landmark

**MF:** MidFoot

**RoM:** Range of Motion

**SCS:** Segment Coordinate System

**SP:** Stance Phase

**STA:** Soft Tissue Artefacts





## Introduction

---

Gait analysis is currently a widespread and useful tool for both clinical practice and biomechanical research. Human movement analysis provides a great deal of information regarding joint and segment kinematics and dynamics [Benedetti et al., 1998]. Most of the studies are focused on the hip and knee joints, often in order to study joint replacement. Over the past two decades, some studies were centered on the foot by means of multi-segment foot model. Kinematic validation has already been realized about models with more than three segments [Leardini et al., 2007; Lundgren et al., 2008]. However, very few studies deal with dynamic analysis and no validation has yet been done [Mac Williams et al., 2003]. Actually, the methodology for dynamic analysis is problematic due to the complex repartition of external mechanical actions.

The present study proposes a gait analysis based on a multi-segment foot model, realized with ten healthy subjects walking at comfortable speed. An original method to distribute the external mechanical actions is proposed and tested. Kinematic and dynamic results are provided and compared with previous studies in order to assess the validity of the method.

As a result of this work, an abstract was accepted to be presented at the 35<sup>th</sup> Congress of Society of Biomechanics in August 2010.

The reference of this work is: SAMSON, W., VAN HAMME, A., DUMAS, R., CHEZE, L. *Mechanical actions in a two-segment foot model: comparison of two methods*, Computer methods in Biomechanics and Biomedical Engineering.(Accepted)





# 1. Anatomical and Biomechanical Notions

## 1.1 Body Planes

The planes used in this study, are the usual planes used in anatomical studies. In Figure 1.1, those three orthogonal planes are represented. Their characteristics are:

- **Sagittal** plane separates body into right and left parts
- **Coronal** or **Frontal** plane separates body into anterior and posterior parts
- **Transverse** or **Axial** plane separates body into superior and inferior parts

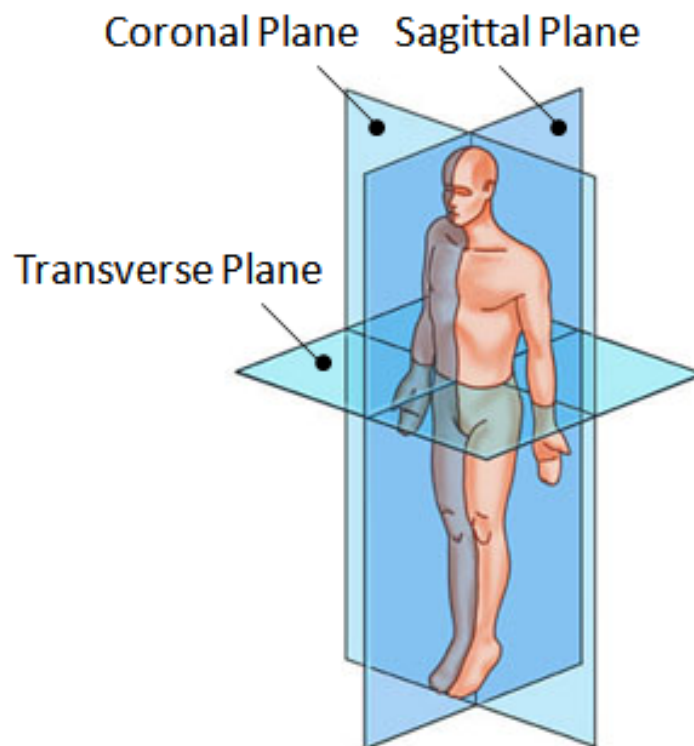


Figure 1.1 - Body planes

It can be noticed that in human gait, motions appear mainly in the **sagittal plane**.



## 1.2 Lower Limb Functional Anatomy

Each lower limb is composed of thirty bones: the femur in the thigh, the patella, the tibia and the fibula in the leg, seven tarsal and five metatarsal bones in the foot and fourteen phalanges in the toes. The lower limb bones are represented in Figure 1.2. The pelvic, or coxal bone, is a flat bone linking the two lower limbs. The femur corresponds to the thigh bone; it is a long bone, the longest of the whole body. It articulates with the coxal bone, at the top and the tibia and patella at the bottom. The patella is a little bone in anterior knee region articulated with the femur. It is situated in the tendon of the femoral quadriceps. The leg is composed of two bones, the tibia and the fibula (both long bones). The tibia is anterior and medial while the fibula is posterior and lateral. The tibia is articulated with femur at the top, talus at the bottom and fibula laterally, whereas the fibula is not articulated with the femur. Then, the foot is composed of three kinds of bones: tarsals, metatarsals, phalanges, which will be more detailed thereafter (section 1.3.1)

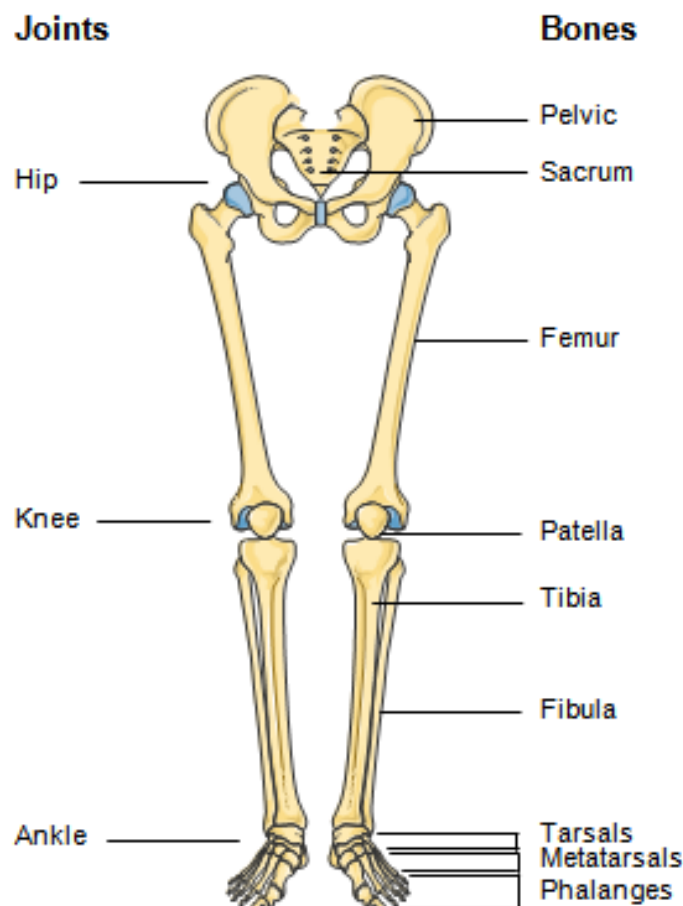


Figure 1.2 - Lower limbs





From top to bottom, inferior limb includes hip joint, knee joint, ankle joint and foot joints.

The **hip** movements are realized thank to the coxofemoral joint (femoral head in the coxal bone cavity). It is a very fitted and resistant spherical joint that allows large movement amplitude. The geometry of these bones leads to its modeling in the form of a spherical joint, (i.e., rotation around the three axes is possible). In the sagittal plane, the movements are flexion and extension, in the frontal plane, the movements are abduction and adduction and in the transverse plane the movements are internal and external rotation.

The **knee** is the joint that unites the three leg bones: femur, tibia and patella. It is a synovial joint composed of two joints: femorotibial and femoropatellar joint. The knee articular cavity is the bulkiest cavity of human body. The principal movements are flexion and extension but combined with some rotation during flexion or extension.

The **ankle** is also called tibiotarsal joint. This joint is indispensable for gait. It is a joint with only one Degree of Freedom (DoF), as long as only movements between the fibula and the talus are considered. Indeed other foot movements are allowed because of the bones in the foot (see section 1.3.2).

### 1.3 Gait Cycle

Human gait analysis referred to the evaluation of the manner or style of walking, by observing and also measuring the human as he walks. A gait cycle (Figure 1.3) is usually defined as the time between two consecutive heel strikes and is composed of two phases. During the Stance Phase (SP), the foot is in contact with the ground while not in the swing phase. In biomechanical research or clinical study, it is currently used a stereophotogrammetric system for the kinematic approach (joint angles) and often forceplates for the dynamics (joint moments).



Figure 1.3 - A Human Gait Cycle



## 1.4 Foot Description

### 1.4.1 Foot Bones

The foot is a complex articular system composed of twenty-six bones. More than fifty ligaments and twenty-three muscles with up to four tendons act on the foot. In agreement with the purpose of the current study, only foot bones are considered.

As it was exposed in section 1.2, foot bones can be classified into three parts: tarsals, metatarsals and phalanges (Figure 1.4).

The **tarsal bones** can be separated in two parts: posterior and anterior. The posterior part of the tarsal bones consists of the talus and the calcaneus. The calcaneus is the largest and strongest tarsal bone. The anterior tarsal bones are the navicular, the three cuneiforms (third = lateral, second = intermediate, first = medial), and the cuboid. The talus is the only bone of the foot articulated with the fibula and tibia. The ankle joint, the proximal region of the foot, is composed on one side of the lateral malleolus of the tibia and on the other side of the medial malleolus of the fibula. During walking, the talus transmits about half the weight of the body to the calcaneus. The remainder is transmitted to the other tarsal bones.

The metatarsus is the intermediate region of the foot and consists of five **metatarsal bones** numbered from I to V from the medial to lateral position. The metatarsals articulate proximally with the cuneiform and the cuboid while distally, they articulate with the proximal row of phalanges. The first metatarsal is thicker than the others because it bears more weight.

The **phalanges** correspond to the distal component of the foot. The toes are numbered from I to V beginning with the great toe, from medial to lateral. The great toe (hallux) has two large heavy phalanges called proximal and distal phalanges. The other four toes have three phalanges each: proximal, middle and distal.



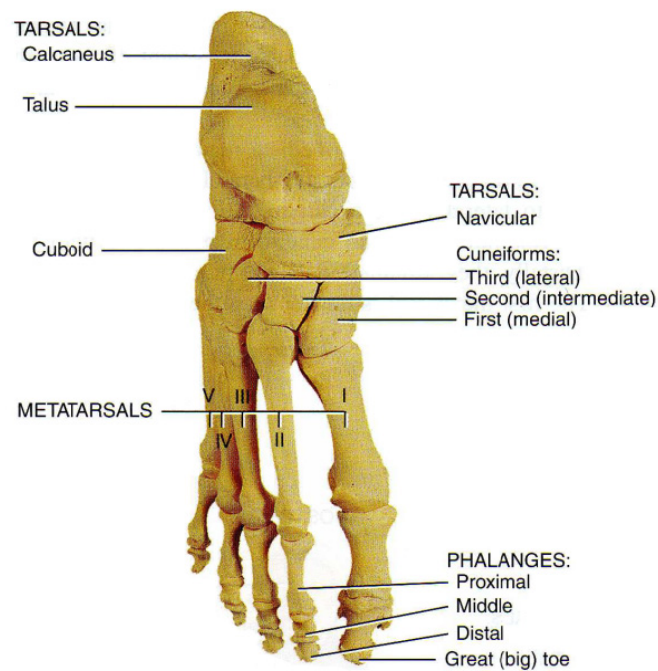


**Figure 1.3 - Foot Bones** (Superior view)

### 1.4.2 Foot Movements

Foot movements are possible thanks to bone geometry and ligaments contribution. In order to describe foot movements, foot articular complex axes are defined (Figure 1.5). The transversal axis  $XX'$  crosses the two malleoli and corresponds to the tibiotarsal joint axis. This axis belongs to the frontal plane and flexion-extension movement in the sagittal plane is realized around this axis. The longitudinal axis  $Y$  of the leg is vertical and supports adduction-abduction movement. The longitudinal axis  $Z$  is horizontal and in the sagittal plane. It conditions the sole foot orientation with respect to the floor, either inside or outside (i.e. pronation-supination movement). The axes intersection is situated at rearfoot area.

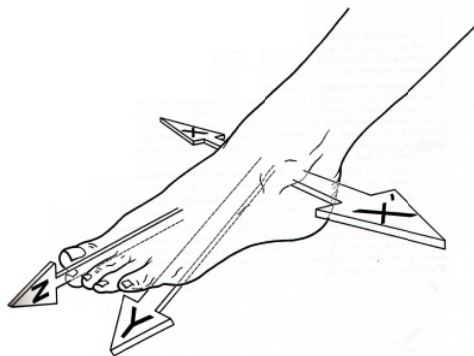


**Figure 1.5 - Foot Axes**



Definitions of the relative movements between the leg and the foot (i.e., the ankle joint) are presented in Table 1.1.

The particular shapes and positions of foot bones allow **movements inside the foot**. More specially, three articular groups can be identified in the foot. The hindfoot is composed of the talus and calcaneum. The talus is part of the ankle joint with the inferior parts of the tibia and fibula. The talus transmits a large part of the body weight between the leg and foot. The calcaneum, located just under talus, is the base of the foot. The Achilles tendon, the strongest tendon of human body, attaches on this bone. Both bones are strongly linked and distribute body weight between floor and the rest of foot.

The midfoot (navicular, cuboid, three cuneiforms) is less mobile than the hindfoot. This part is composed of transmission arches between hindfoot and forefoot.

The forefoot (five metatarsals and toes) is the latest foot part. The two longitudinal arches are there. They are responsible of the end of the braking phase, stabilization of stance and transmit propulsion force to the floor. The foot extremity consists of toes composed of phalanges (two for hallux and three for the others). These phalanges distribute body weight during stance phase. The first and second toes are useful for propulsion.









	Flexion/ Extension		Adduction / Abduction		Supination / Pronation	
Rotation axis	XX'		YY'		ZZ'	
Name	Flexion	Extension	Adduction	Abduction	Supination	Pronation
Description	when foot close in from the leg (dorsi-flexion)	when foot moves away from the leg (plantar-flexion)	Tiptoe inside, toward symmetric body plane	Tiptoe outside, move away from symmetric body plane	Sole towards Inside	Sole towards Outside
Amplitude in degrees	20 to 30	30 to 50	35 to 45 if we consider movement in foot only (until 90 if couple with knee)		45 to 50	25 to 30
Picture						
Notes	In extreme position, the movement is possible with contribution of tibiotarsal and tarsus joints.		This movements never occur separately but always combined			
Inversion is composed of:		+	+		+	
Eversion is composed of:	+			+		+

Table 1.1 - Foot Movements





## 2. State of the art – Problematic

---

### 2.1 State of the Art

Gait analysis is often used in various fields: clinics –in order to check surgical intervention usefulness or to detect anatomical anomalies–, sports –to control training program effects– and commercial –optimization of shoe design corresponding with foot anatomy and gait requirements–. Therefore, a lot of studies deal with this topic. Most of the studies are focused on the principal lower limb joints that are the hip and the knee and consider the foot as a single rigid segment [Kadaba et al., 1989]. Recently, some authors developed a foot model segmented in different parts in order to consider motion in the multiple joints of the foot. This multi-segmented modeling allows the specific study of foot abnormalities as rheumatoid arthritis [Woodburn et al., 2002], posterior tibial tendon dysfunction [Rattanaprasert et al., 1999], arthrodesis [Wu and Cavanagh, 1995], ankle fracture [Wang et al., 2009] and ankle prosthesis [Ingrosso et al. 2009]. Some of the studies are based on an invasive protocol [Arndt et al., 2007] not possible in our case due to ethical reasons.

Moreover, dealing with gait analysis, it is compulsory to respect International Society of Biomechanics (ISB) recommendations (2002) for segments' location. This paper was written in order to harmonize gait analysis studies and facilitate understanding and comparisons. However, there is no ISB recommendation specific to foot segmentation.

Furthermore, the lower limb model currently used in the laboratory (*Laboratoire de Biomécanique et Mécanique des Chocs*, supervised by L. Chèze) is a classical model validated for global gait analysis (hip or knee pathologies), but it is not adapted for ankle or foot pathologies, due to the foot modeled as a single segment.

Very few studies include dynamics. Stefanyshyn and Nigg (1997) calculated the metatarsophalangeal moment only when the Ground Reaction Force (GRF) is distal to the joint. Mac Williams et al. (2003) proposed a more complete model based on the repartition of the GRF on the different foot segments.

These considerations reinforce the double interest of the present study: from kinematic and dynamic points of view.



### 2.1.1 Existing Models

Various multi-segmented models have been developed. Some of them, composed of two [Moseley et al., 1996] to nine segments [Mac Williams et al., 2003], will be shown. At the end of this section, Table 2.1 compiles models and their characteristics in order to make the comparison easier.

Early foot models focused on the motion of the HindFoot (HF) relative to the tibia [Moseley et al., 1996; Kepple et al., 1990]. The only foot bone observed in these studies is the calcaneum. These models allowed confirming some assumptions for global foot movement (the real existence of a mechanical coupling between the rearfoot abduction/adduction and eversion/inversion movements). However, this modeling is not sufficient for the study of more precise foot kinematics and dynamics.

By means of a three-segment foot model composed of Tibia, HF and ForeFoot (FF), Hunt et al. (2001) underlined that foot segmentation is necessary in order to study foot movements, as they obtained non negligible movements between HF and FF.

In order to observe the effects of surgical intervention following ankle fractures, Wang et al. (2009) used a model with the three segments Tibia, HF and FF and considered the Hallux (HX) as a vector but not a segment.

The study of Carson et al. (2001) aimed to establish a standardized protocol to analyze foot kinematics. However, the first results obtained required thorough testing and validation. Here, interest in the mid-foot focused on its role as a mechanism transmitting motion between the HF and forefoot. This model is known as “The Oxford model”. A possible representation is on Figure 2.1. Myers et al. (2004) used also this model to validate a protocol for children gait analysis.

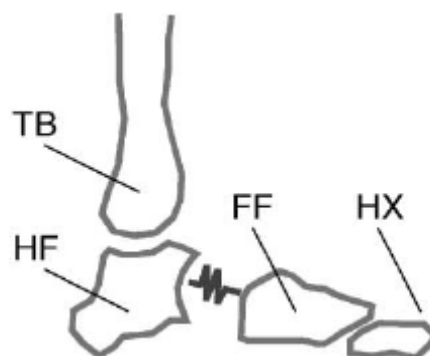
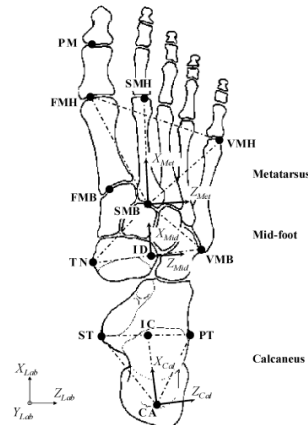


Figure 2.1 – Oxford Foot Model





Leardini et al. (2007) developed an original method considering the foot as four segments (Tibia, Calcaneus, MF, Metatarsals – Figure 2.2). During the data analysis phase, they observed movements within the foot and also movements of the entire foot with respect to the leg. This allows having a complete analysis of the foot and is available for comparison with a large range of studies. However, they used angles projection method, with HX, metatarsal I, II and V assumed as independent line segments restricting angular information.



**Figure 2.2 – Leardini Foot Model**

Jenkyn and Nicol (2007) defined various kinematic parameters: ankle and subtalar joints DoF, frontal and transverse plane motions of the HF relative to MF, supination/pronation twist of the forefoot relative to MF and medial longitudinal arch height-to-length ratio. This multi-segment foot model allows to measure motion within the foot but dynamics is not addressed.

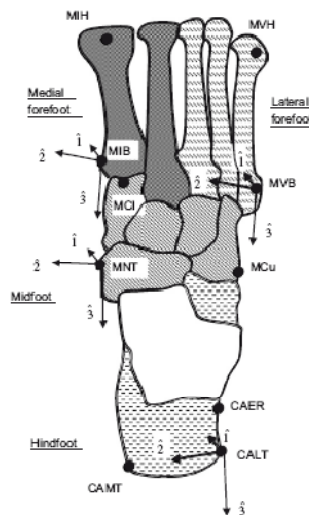


**Figure 2.3 – Jenkyn Foot Model**



Simon et al. (2006) described the Heidelberg model as a foot model based on projection angles measured between “functional segments”. These segments were defined by markers (Figure 2.4) and encompassed multiple bones and articulations similar to segments labeled as rigid body segments in the previously discussed models. However, the Heidelberg model uses projection angles to describe angular motion of the joints, and thus do not allow assessing a three-dimensional information.

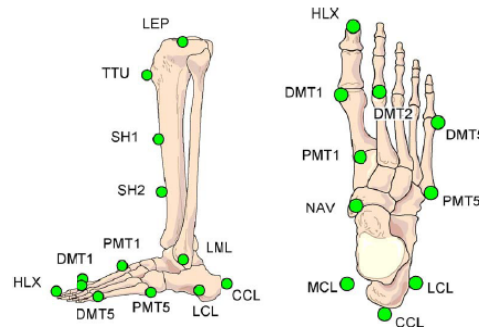


**Figure 2.4 – Heidelberg Foot Model**

The model with most segments is the one developed by Mac Williams et al. (2003). They proposed a foot segmented in nine functional units by means of nineteen markers. The results indicate that single link models of the foot significantly overestimated ankle joint powers during gait. The authors defined the actions on each functional unit by distributing the forceplate data under each foot segment using a plantar pressure plate. The authors hypothesized that shear forces and twisting moments are distributed among each segment in proportion to the normal force. The validation for the kinematics is presented but there is no information about an eventual dynamic validation.

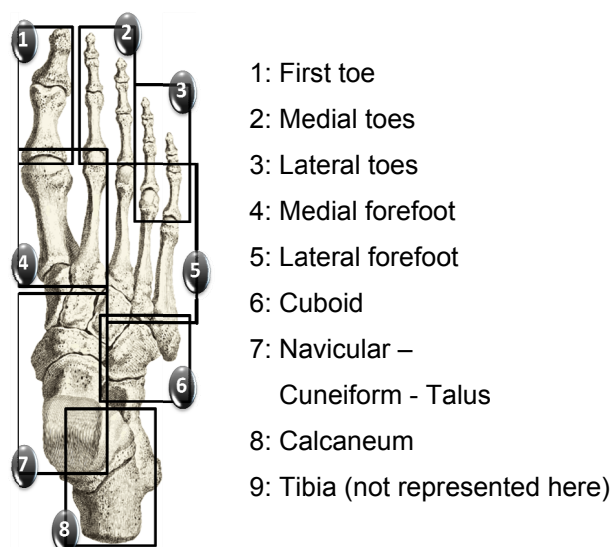


**Figure 2.5 - Mac Williams Foot Model**



### **2.1.2 Source of Errors**

Doing experimental measurements, sources of errors affect photogrammetric measurements and then marker coordinates [Chiari et al., 2005]. Errors are unpredictable (due to the instrumentation) or systematic (coming from experimental method).

In order to minimize the instrumentation errors and increase the three-dimensional measurement precision, it is necessary to cautiously calibrate the capture volume. In the present study, a double calibration (static and dynamic) of the Motion Analysis<sup>®</sup> system has been done (section 3.1.1). Besides, the order of magnitude of these errors is largely inferior to the experimental ones.

From the experimental part, Gorton G. et al. (2001) exposed that a very important parameter is the marker placement which can be different for the different subjects. In order to limit this, it is required that the same operator who places the markers for all the subjects involved in the study.

Another source of errors is the presence of Soft Tissue Artefacts (STA) brought by the soft tissue present between the skin marker and the real anatomical position of the studied bone. Some methods have been proposed to address this problem; these are exposed in section 2.2.3.

### **2.1.3 Correction Methods**

#### **Solidification Procedure**

When skin markers (measurement points) are used in gait analysis, the presence of STA is unavoidable. Chèze et al. (1995) proposed a solidification procedure to reduce the STA. However, treating with foot movements, it is possible to consider that STA are reduced because it is a region with few soft tissues, therefore, this step will not be considered.

#### **Invasive Method**

Another method, surely more efficient but obviously difficult to realize with respect to ethical problematic, consists in using intracortical pins, implanted during a surgical intervention. An example of instrumented foot is represented in Figure 2.6.



In the study of Arndt et al. (2007), the segment motion relative to adjacent proximal segments was determined using helical axes projected into the coordinate system of the proximal segment. Coefficients of Multiple Correlation, calculated to determine the strength of association between running style with and without the inserted pins, indicated that the subjects had little restriction due to the inserted pins. The study showed frontal plane rotation of the talocrural joint, which exceeded that of the subtalar joint. Considerable mobility of the talonavicular joint was found. Furthermore, small, but non-negligible motion between the fibula and tibia was observed.

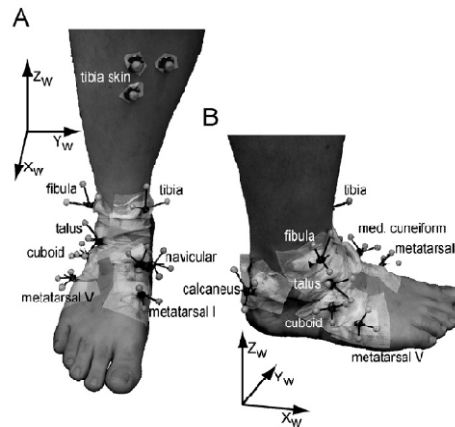


**Figure 2.6 – Invasive Markers** (Arndt 2007)

In another field, Nester (2009) experimented with cadavers and compared results with in-vivo previous studies. The conclusions were that the rearfoot is only a part of overall foot kinematics and that contribution from mid- and forefoot articulations have been consistently underestimated. The forefoot undergoes a complex series of rotations which must influence the action of the intrinsic muscles of the foot. Also, it is specified that variation between people in foot kinematics is high and normal.

### **Plate mounted markers**

Another technique exists for reducing skin movement artefacts. It consists of using plate mounted markers like in Benedetti et al. (1998) and Leardini et al. (1999). The location of plate mounted markers is illustrated in Figure 2.7. This method allows obtaining satisfying results of repeatability of rotation measurements. Furthermore, plate mounted markers present advantages since “it can embrace the underlying bones better than skin-mounted markers. Additionally, the cluster orientations allow a limited number of cameras while ensuring adequate views of the markers throughout the entire stance phase. The analyzed subjects did not claim any disturbances to their normal walking by the measuring set-up”.

[Leardini et al., 1999]





**Figure 2.7 - Plates Mounted Markers**

Location of the retroreflective markers mounted on plexiglas plates. The drawing also shows the calibration of the apex of the tuberosity of the cuboid landmark using the pointer

### Marker attachment method comparison

Nester et al. (2007) compared with a four-segment foot model (HF, MF, Medial FF and Lateral FF) the three markers fixation methods: directly on skin, with plates and intracortically. They captured three kinds of trials (Figure 2.8) for each subject.

Due to the obligation of collecting data in three separate testing sessions, it is not possible to provide a clear answer whether one method is preferable than the others. There are no significant differences in articular nor in plane movements. No conclusion can be drawn, especially for comparison between skin and plates protocols. Besides, the problem is surely more in the rigid segment modeling rather than in the attachment protocol.

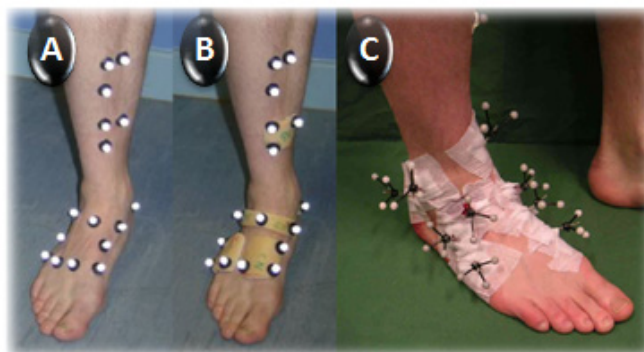


**Figure 2.8 - Methods Compared**

- A: Skin mounted markers
- B: Plate mounted markers
- C: Bone pins inserted in nine bones of the foot



#### 2.1.4 Normalized Moments

When joint moments are calculated, it is necessary to normalize them dimensionless, in order to compare subjects. The most common way to do this is to divide the value of the moments by the subject body weight [Benedetti et al., 1998] or the subject mass [Mac Williams et al., 2003]. A recent study [Samson et al, 2010] proposed to make the moments dimensionless with the product of body weight by the length of the leg with young children. Nevertheless, there is no consensus regarding this aspect.



### 2.1.5 Synthesis Table

Article	Segments	Studied Movements	Markers Position for each segment (except Tibia)	Remarks
<b>Hunt et al.</b> <b>(2001)</b> <i>Adults Gait</i>	- Tibia - RF - FF	- HF et RF motions - Medial longitudinal arch height	1) HF : Calca post, Calca Ext, Calca Int 2) FF: BM5, HM5, HM1	Coordinate systems in order to calculate movements of 2 adjacent segments but not clearly explained.
<b>Wang et al.</b> <b>(2009)</b> <i>After fracture ankle interventions</i>	- Tibia - HF - FF - HX (Vector)	- Tibia/HF Flexion - Tibia/HF Rotation -Tibia/HF Inversion - Tibia/FF Flexion - Tibia/FF Pronation - Tibia/FF Abduction - HF/FF Flexion -HF/FF Rotation	1) HF : Calca post, Calca ext, Calca int 2) FF : BM1, HM1, BM5, HM5 3) HX : Hallux	- MF assumed as a mechanism transmitting movements between HF and FF. - HX Varus/Valgus, measured between HX vector and its projection in FF sagittal plane - Model used : the one described by Stebbins
<b>Carson et al.</b> <b>(2001)</b> <i>Adults Gait</i>	- Tibia - HF - FF - HX	- Tibia/Floor - HF/Tibia - FF/HF - HX/FF	1) HF : Calca post, Calca ext, Calca int 2)FF : HM1, BM1, HM5, HM1 3) HX : Triad	- This model is named Oxford Model - HM1, removed for dynamic trials because of important skin movements.



<b>Myers et al.</b> <b>(2004)</b>  <b>Children</b> <b>(6-11 years)</b>	<ul style="list-style-type: none"> <li>- Tibia-Fibula</li> <li>- HF</li> <li>- FF</li> <li>- HX</li> </ul>	<ul style="list-style-type: none"> <li>- Tibia / Floor</li> <li>- Tibia /HF</li> <li>- HF/FF</li> <li>- FF/HX</li> </ul>	1) HF : Talus, Navicular, Calcaneus 2) FF : Cuboid, Cuneiforms, Metatarsals 3) Hallux	<ul style="list-style-type: none"> <li>- Euler angles method for angular rotation calculation</li> </ul>
<b>Leardini et al.</b> <b>(2007)</b>  <b>Adults Gait</b>	<ul style="list-style-type: none"> <li>- Tibia</li> <li>- HF</li> <li>- MF</li> <li>- FF</li> <li>- HX</li> </ul>	<ul style="list-style-type: none"> <li>- Shank/Foot</li> <li>- Shank/HF</li> <li>- HF/MF</li> <li>- MF/ FF</li> <li>- HF/FF</li> </ul>	1) HF : Calcaneum 1bis) Entire foot 2) MF : Navicular et 3 cuneiforms 3) FF : 5 metatarsals 3bis) HX, M1, M2 et M5 assumed as independant segments	<ul style="list-style-type: none"> <li>- HX results not exposed</li> <li>-Influence of markers set choice not very important for data analysis (Stebbins 2006)</li> <li>- They give landmarks definition but not exactly the markers position</li> </ul>
<b>Jenkyn et al.</b> <b>(2007)</b>  <b>Adults Gait</b>	<ul style="list-style-type: none"> <li>- Tibia</li> <li>- HF</li> <li>- MF</li> <li>- Nav-Cub</li> <li>- Medial FF</li> <li>- Lateral FF</li> </ul>	<ul style="list-style-type: none"> <li>- Ankle motion flexion</li> <li>- Subtalar motion inv/eve (talus head defined on MF et lateral tuberosity – Achille tendon fixation- defined on MF)</li> <li>- HF/MF supination</li> <li>- HF/MF rotation</li> <li>- FF/MF supination</li> </ul>	1) HF : Calcaneum 2) MF : 3 cuneiforms 3) navicular, cuboid 4) Medial FF : HM1, BM 5) Lateral FF : HM5,BM5	<ul style="list-style-type: none"> <li>- HX not considered here.</li> <li>- Talus not tracked, reconstituted using adjacent segments.</li> </ul>





<b>Simon et al. (2006)</b>  <b>Heidelberg Model</b>	Not exposed in details	<ul style="list-style-type: none"> <li>- Talus flexion</li> <li>- Medial arch inclination</li> <li>- Medial arch</li> <li>- Lateral arch</li> <li>- Subtalar inversion</li> <li>- FF/Ankle Supination</li> <li>- FF/MF Supination</li> <li>- FF/HF Abduction</li> <li>- FF/Ankle Abduction</li> <li>- MTI-MTV Angle</li> <li>- HX Flexion</li> <li>- HX Abduction</li> </ul>	Markers positions (Segments not exactly defined) :  <ul style="list-style-type: none"> <li>- Calca post</li> <li>- Calca ext</li> <li>- Calca Int</li> <li>- Navicular</li> <li>- Between cuneiform 1 and meta 1</li> <li>- HM1</li> <li>- HM2</li> <li>- HM5</li> <li>- BM5</li> <li>- HX</li> </ul>	<ul style="list-style-type: none"> <li>- Details about determination of lateral calcaneus position because they are not palpable.</li> <li>- Landmarks selected description and projection angles method</li> <li>- Talus representation with markers on calcaneum is validated for ankle movements' observation because principal movement: subtalar rotation.</li> </ul>
<b>Mac Williams et al. (2003)</b>  <b>Adolescent Gait</b>	<ul style="list-style-type: none"> <li>- Tibia</li> <li>- Calcaneum</li> <li>- Cuboid</li> <li>- Tal-Nav-Cune</li> <li>- Lateral FF</li> <li>- Medial FF</li> <li>- Lateral Toes</li> <li>- Medial Toes</li> <li>- HX</li> </ul>	<ul style="list-style-type: none"> <li>- Tal-Nav Cune/Tibia - -Fib</li> <li>- Calca/ Tal-Nav-Cune</li> <li>- Calca/Cuboid</li> <li>- Medial FF/Tal-Nav-Cune</li> <li>- Lateral FF/Cuboid</li> <li>- Lateral Toes/Lateral FF</li> <li>- Medial Toes/Medial FF</li> <li>- HX/Medial FF</li> </ul>	1) Calca : Calca post, Calca ext, Calca Int 2) Lateral FF :HM3,BM3, HM5, BM5 3) Medial FF : HM1, BM1 4) Lateral Toes : 5 <sup>th</sup> distal phalange 5) Medial toes : 2 <sup>nd</sup> distal phalange 6) HX : Triad	No marker in cuboid and Tal-Nav-Cune, but their movements are observed.



<b>Arndt et al.</b> <b>2007</b> <i>Slow running</i> <i>(intracortical)</i>	<ul style="list-style-type: none"> <li>- Fibula</li> <li>- Tibia</li> <li>- Talus</li> <li>- Calcaneum</li> <li>- Cuboid</li> <li>- Navicular</li> <li>- Cuneiform</li> <li>- Metatarsal I</li> <li>- Metatarsal V</li> </ul>	<ul style="list-style-type: none"> <li>- Talus/Tibia</li> <li>- Calca/Talus</li> <li>- Nav/Talus</li> <li>- Cub/Calc</li> <li>- Cub/Nav</li> <li>- Cun/Nav</li> <li>- Meta1/Cun</li> <li>- Meta5/Cub</li> <li>- Tibia/Fib</li> </ul>	<ul style="list-style-type: none"> <li>1) Talus</li> <li>2) Posterior calcaneum</li> <li>3) Cuboid</li> <li>4) Navicular</li> <li>5) Medial cuneiform</li> <li>6) BM1</li> <li>7) BM5</li> </ul>	<ul style="list-style-type: none"> <li>- Medium repeatability</li> </ul>
<b>Leardini et al.</b> <b>(1999)</b> <b>Plates</b> <b>Mounted</b> <b>Markers</b>	<ul style="list-style-type: none"> <li>- Tibia</li> <li>- HF</li> <li>- MF</li> <li>- FF</li> <li>- HX</li> </ul>	<ul style="list-style-type: none"> <li>- Tibia/HF</li> <li>- HF/MF</li> <li>- MF/FF</li> <li>- FF/HX</li> </ul>	<ul style="list-style-type: none"> <li>1)HF :Lateral apex of Peroneal Tubercle, most medial projection of Sustentaculum Tali, Calca Post</li> <li>2) MF : Navicular, Cuboid, Medial Cuneiform</li> <li>3) FF : Base, Medial Head, Meta 1 Lateral Head</li> <li>4)HX : triad</li> </ul>	<ul style="list-style-type: none"> <li>- Important repeatability</li> <li>- Determination of landmark points with markers projection</li> <li>- Plates Advantages: Less influence of skin movements / In contradiction with Nester article (less kinematic errors but not skin movements)</li> </ul>

Table 2.1 – Foot Models Synthesis Table



## **2.2 Problematic**

A lot of studies have developed multi-segment foot models in order to characterize foot kinematics. Recent technology evolution (improvements in camera resolution) allows the use of smaller markers, considering the demarcation of more and smaller segments of the foot. This modeling is commonly used and quite well validated for kinematics analysis. However, few dynamic studies exist and even fewer dynamic validation. The difficulty of computing dynamic data for a multi-segment foot comes from the measurement of external actions: a forceplate measures GRF considering the foot as a whole. Therefore, MacWilliams et al. (2003) proposed to use plantar pressure plate combined with forceplate in order to distribute external actions among the foot segments. The method assumes the hypothesis that shear forces and twisting moments are distributed among each segment in proportion to the normal force. This method has not yet been validated. Therefore, another original method of external actions distribution based on Coulomb's laws [Samson et al., 2010] will be used in the present study, and result comparison will be done.

The present protocol will be tested on healthy subjects, in order to build a reference database, which is a first essential step for future pathologic cases study.





## 3. Materials and Protocol

### 3.1 Materials

Instrumentation materials were situated in the laboratory of the Medicine Faculty in Pierre Bénite, close to Lyon. It is the combination of three elements that permitted this study. It is important to notice that time synchronization between all instruments is compulsory.

A **gait analysis system** is composed of a cluster of cameras that captures the movement of markers in its field of view. A software is compulsory for three-dimensional trajectory reconstructions from optical measurements. The cameras and the software give the kinematic information of the gait trial. Then, to get dynamic data, the addition of forceplates permits to measure GRF when the foot is in contact with it during SP. Finally, baropodometric plate can give pressure information when the subject walks on it. The Figure 3.1 presents the laboratory where measurements were completed.



**Figure 3.1 - Laboratory Disposition**

- A: Eight Infrared Cameras
- B: Two Forceplates
- C: One Baropodometric Plate



### 3.1.1 Motion Analysis® System

A Motion Analysis® System with eight Eagle® Cameras (Santa Rosa, USA) was used. It is a high resolution and high frequency system allowing obtaining a resolution of 1200 x 1024 pixels with a frequency of 500 Hz. For the study, the frequency was set to 100 Hz, with the maximum resolution.

Cameras emit infrared light, retroflected by markers covered by a special material named ScotchLigh®. Two kinds of spherical markers (Figure 3.2) were used: 0.25" (9,525 mm) in diameter without plastic base (fixed on the skin with physiological double face scotch-tape), and 0.75" (19,05 mm) in diameter fixed on a plastic base.

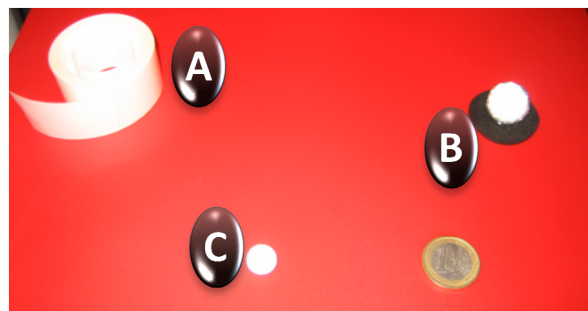


**Figure 3.2 – Markers**

A: Physiological adhesive tape  
B: 0.75" marker  
C: 0.25" marker

Frames are digitized and computed with a stereophotogrametric software (Cortex®)

A very important preliminary phase is **calibration** which enables doing the most precise measurements. It aims to define the cameras characteristics (position, orientation, focal length...) in order to then allow calculating markers' trajectories in three dimensions. It is composed of two calibration phases: static and dynamic.

Static calibration: With a square of known dimensions (Figure 3.3)

The square is located in a known reference position, a corner of the forceplate. This defines the Laboratory Landmark (LL). You have to check that each camera is only recording 4 points. If there are more than four points, some masks have to be added to delete this parasite point (and so ignore the corresponding volume during the capture). This step allows a first estimate of unknown cameras parameters.

Dynamic phase: With a wand of known dimensions (Figure 3.4)

The operator scans with the wand the capture volume, waving the wand in this volume. It is



important to scan the whole volume with the wand, in order to get the best accuracy and to homogenize the accuracy in all the field of view. This phase permits to correct errors of each camera, errors due to optic objective imperfection. In addition, this phase is useful to improve the identification of cameras parameters in the LL.

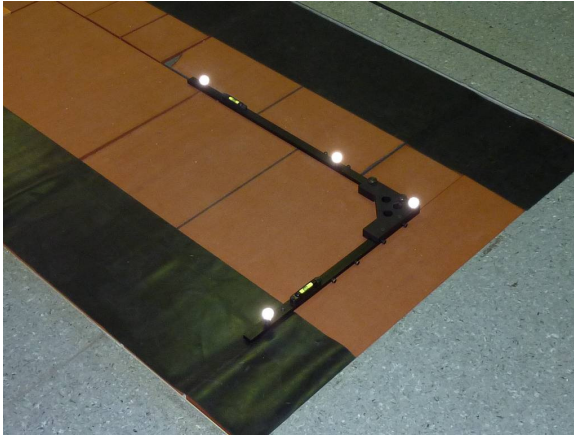


**Fig 3.3 – Calibration Square**

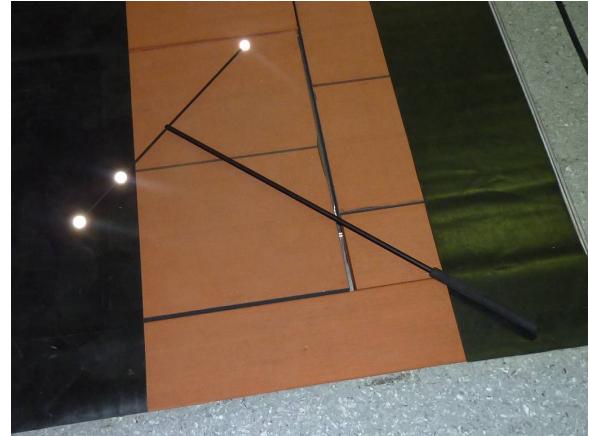


**Fig 3.4 – Calibration Wand**

This gait analysis system presents advantages related to the use of retro-reflective markers letting subject free from movement constraints (in opposition to other technologies that require wires supplying energy to the markers). Nevertheless, the cameras positioning has to be very cautious because each marker have to be seen by at least two cameras in order to make the calculation of its trajectory possible.

### **3.1.2 Force Plates**

The forceplates used are two Bertec<sup>®</sup> forceplates (Colombus, USA) having for dimensions 400 mm x 600 mm and an acquisition frequency of 1000 Hz.

This analogical acquisition system measures contact actions between the foot and the ground. It gives reaction forces and moments at the centre of the forceplate, expressed in the three principal axes. It is composed of four piezoelectric sensors fixed on two rigid metallic bases. One base is fixed; the other is mobile and bears constraints, which are transmitted to sensors. The measurements are amplified and then combined to give force components on the three axes defined by forceplate constructor (Figure 3.6). The moment values at the platform center and the center of pressure are also available. The synchronization between the cameras and forceplates is possible by mean of one master camera with a special plugging. The forceplates and the measured forces are visualized in the stereophotogrametric software.





### 3.1.3 Plantar Pressure Plate

One Footscan® plantar pressure plate (Olen, Belgium) having for dimensions 1068 mm x 418 mm x 12 mm and a frequency of 500 Hz is also used.

The plate is composed of a resistive sensor matrix (128 x 64 sensors) which measures vertical force in each sensor. The sensor surface known, and using the Eq. 3.1, it is easy to determine the foot plantar pressure.

$$P = \frac{F}{S} \quad \text{Eq. 3.1}$$

Where:

- P: Pressure [MPa]
- F: Force [N]
- S: Surface [mm²]

The data treatment is done by RsScan® software. The output data is the dynamic roll off, which will be useful for the determination of the different sections during stance phase (SP) e.g. when the foot is in contact with the floor.

The figure 3.5 sums up the different data available from the laboratory:

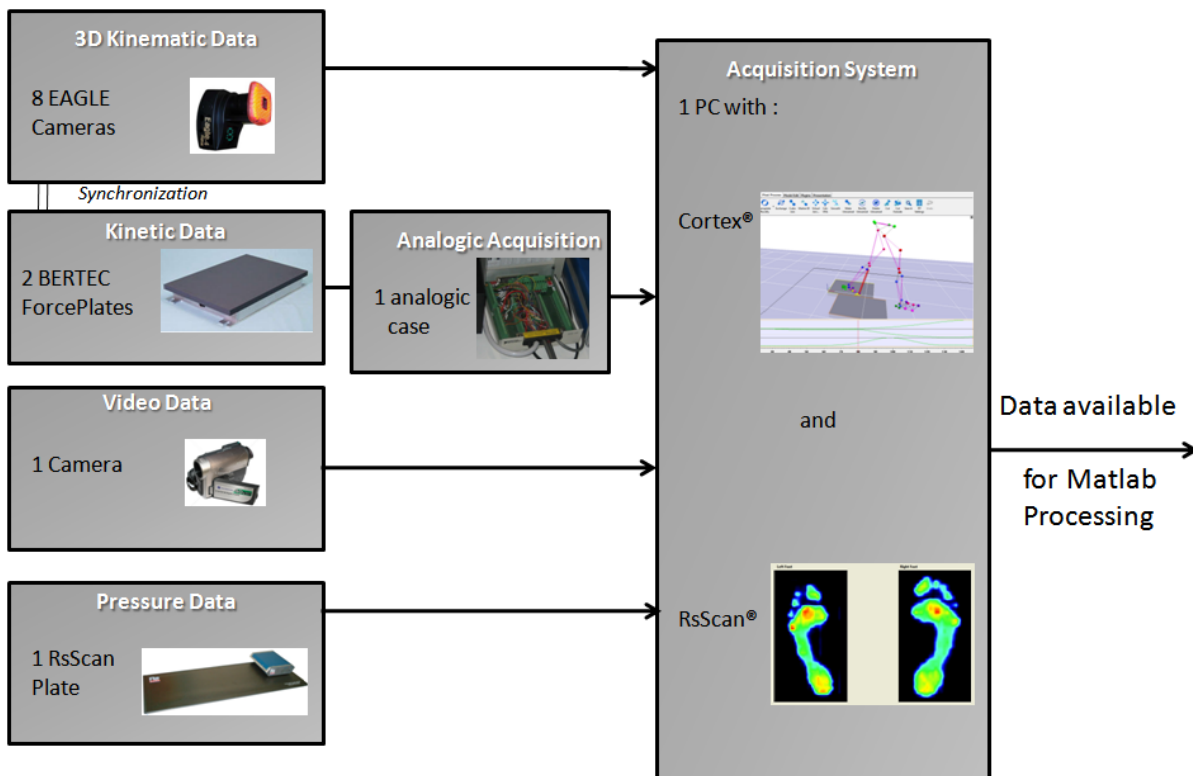


Figure 3.5 – Data Available





### 3.1.4 Landmarks Definition

Because of different element disposition in the laboratory and in order to respect the ISB recommendation, different landmarks are used. They are presented in the Figure 3.6:

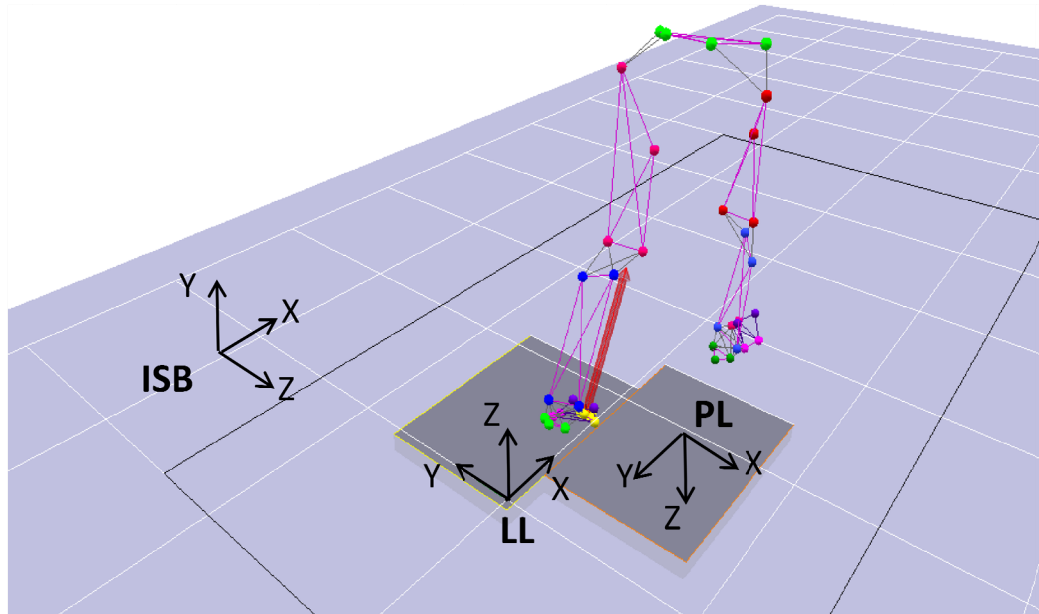


**Figure 3.6 – Landmarks (Cortex®)**

ISB: International Society of Biomechanics Landmark  
LL: Laboratory Landmark  
PL: Forceplates Landmark

## 3.2 Protocol

### 3.2.1 Preparation and Subject Trials

Due to the important number of markers on the foot, we have to evaluate the positioning of the eight laboratory's cameras in order to have the best possible measurements. Then, the calibration phase is realized as described in section 3.1.1.

Next, the markers are placed by palpation of anatomical landmarks. The importance in markers placement is not that much focused on anatomical reliability but more on reproducibility of positions on all subjects in order to make the comparisons meaningful. The placement of markers on the subject is illustrated in Figure 3.7.

Then, the subject has to walk at comfort speed. A couple of trials are executed so that the subject can adapt itself to the environment, and to determine the distance between the point of departure and foot position on plates. When the subject is ready for the measurement, the



motion capture can begin. It is composed of five trials with the right foot on the force plate and five others with the left foot. During the trial, the subject walks also on the baropodometric plate, situated few meters behind forceplates.

Moreover, circumduction trials are recorded; one with each leg in order to determine the hip joint center. That allows having more precision in the determination of the hip joint center than using a regression method. A circumduction is an active or passive circular movement, around a fixed point or axis. In the case of the hip, it consists of being on one leg and doing small circles with the other extended leg. We used the circumduction method described in Ehrig et al. (2006) in which it is specified that the segments have to rotate more than approximately  $20^\circ$  with respect to the adjacent segment to neglect errors due to the algebraic method (if the RoM is too small, errors are too large).

All trials are also recorded with conventional video camera in order to have a reference during data treatment with the software.

Ten healthy subjects (two women and eight men; age =  $29 \pm 6$  years old; weight:  $74 \pm 18$  kg; height:  $174 \pm 10$  cm) were enrolled in the present study. Subjects do not present specific lower limb pathology.



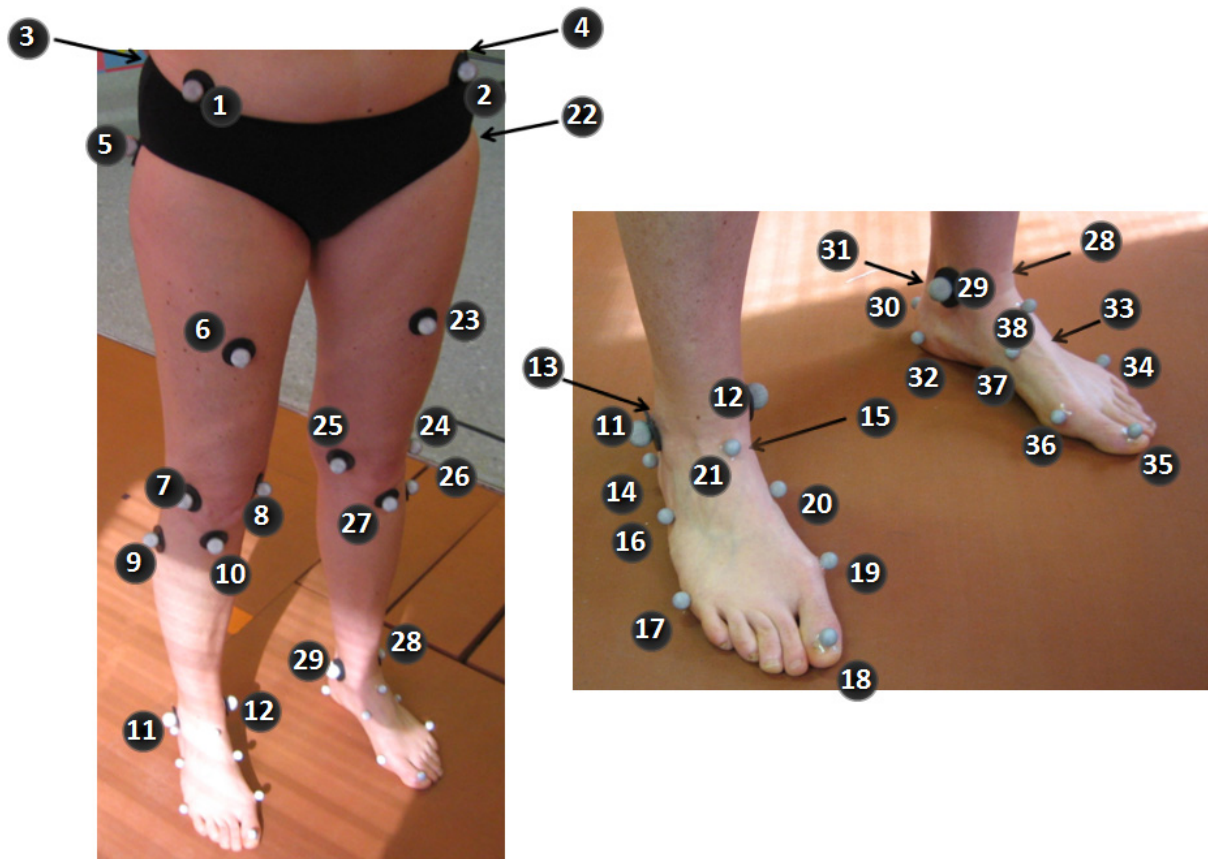


Figure 3.7- Markers Position

- |   |   |
|---|---|
| 1. ASIS_R: Right Anterior Superior Iliac Spine  | 22. GT_L: Left Greater Trochanter           |
| 2. ASIS_L: Left Anterior Superior Iliac Spine   | 23. Thigh_L: Left Thigh                     |
| 3. PSIS_R: Right Posterior Superior Iliac Spine | 24. Cond_E_L: Left External Femoral Condyle |
| 4. PSIS_L: Left Posterior Superior Iliac Spine  | 25. Cond_I_L: Left Internal Femoral Condyle |
| 5. GT-R: Right Greater Trochanter               | 26. Fibula_L: Head of the Left Fibula       |
| 6. Thigh_R : Right Thigh                        | 27. TTA_L: Left Tibial Tuberosity Anterior  |
| 7. Cond_E_R: Right External Femoral Condyle     | 28. Mal_E_L: Left External Malleolus        |
| 8. Cond_I_R: Right Internal Femoral Condyle     | 29. Mal_I_L: Left Internal Malleolus        |
| 9. Fibula_R :Head of the Right Fibula           | 30. Calca_P_L: Left Posterior Calcaneum     |
| 10. TTA_R : Right Tibial Tuberosity Anterior    | 31. Calca_E_L: Left External Calcaneum      |
| 11. Mal_E_R: Right External Malleolus           | 32. Calca_I_L: Left Internal Calcaneum      |
| 12. Mal_I_R: Right Internal Malleolus           | 33. BM5_L: Base of the Left Metatarsal V    |
| 13. Calca_P_R: Right Posterior Calcaneum        | 34. HM5_L: Head of the Left Metatarsal V    |
| 14. Calca_E_R: Right External Calcaneum         | 35. To_L: Left big toe                      |
| 15. Calca_I_R: Right Internal Calcaneum         | 36. HM1_L: Head of the Left Metatarsal I    |
| 16. BM5_R: Base of the Right Metatarsal V       | 37. BM1_L: Base of the Left Metatarsal I    |
| 17. HM5_R: Head of the Right Metatarsal V       | 38. Nav_L: Left Navicular                   |
| 18. To_R: Right big toe                         |   |
| 19. HM1_R: Head of the Right Metatarsal I       |   |
| 20. BM1_R: Base of the Right Metatarsal I       |   |
| 21. Nav_R: Right Navicular                      |   |



### 3.2.2 Data Tracking

The data treatment is realized with two softwares: Cortex<sup>®</sup> for kinematic and dynamic data and RsScan<sup>®</sup> for baropodometric data.

On one hand, the tracking phase with **Cortex<sup>®</sup>** is composed of different phases:

- Loading Project (files with markers definition and calibration information)
- Loading Track files (one gait trial)
- Labeling of each marker during all the trial. It is not necessary to identify each marker for each frame, because of an automatic rectification by the software which follows one marker in all the trial starting with the reference frame used for marker identification (with foot flat generally). This requires giving some “elasticity” to the links between markers that is defined in assessment with anatomical data. Nevertheless, sometimes the software can not follow the marker during all the trial. Therefore, the operator has to check frame by frame that all markers are identified, and if not, he has to link the unnamed marker corresponding with the treated marker. If some markers are missing, and if there is no unnamed marker recognized in the corresponding frames, marker reconstruction is possible by two methods: reconstruction based on three others markers that belongs to the same segment with positions known and virtual reconstruction (cubic interpolation).
- Application of a filtering. The method used in Cortex<sup>®</sup> is a butterworth that is convenient for gait analysis. The cut-off frequency is adjusted at 6 Hz, as it is widely used in the literature for gait analysis [Houck et al., 2008]. Thus, the errors due to instrumentation (acquisition noises) are reduced.
- Selection of frames corresponding to one gait cycle (from heel strike to heel strike) and exportation (in .trc files) of these selected frames.
- Exportation of .anc files, forceplate data corresponding to selected frames of one gait cycle.

Then, you have one .trc file with kinematic data (numerical) and one .anc file with dynamic data (analogical), needed for post-processing using the Matlab<sup>®</sup> software.



On the other hand, the baropodometric data is not treated with Cortex<sup>®</sup> software but with **RsScan<sup>®</sup>** software, which is specific of the baropodometric platforms. This software provides foot map pressure as it is represented in Figure 3.8.

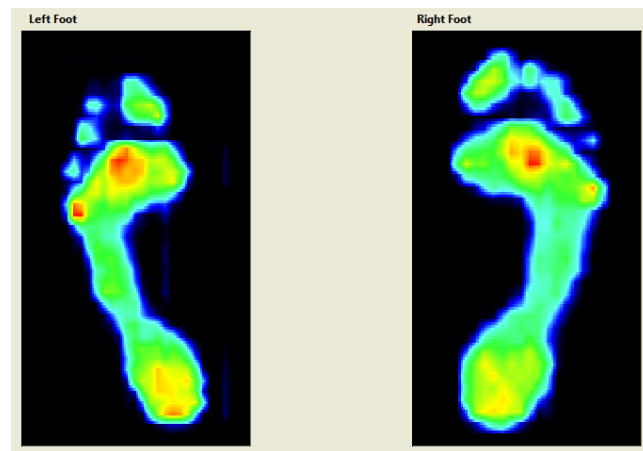


**Figure 3.8 – RsScan<sup>®</sup> Pressure Map**

This software allows obtaining the dynamic roll-off of the foot during stance phase. The exported data are files in .xls format composed of different matrices that represent the pressure value of each sensor of the platform for each image captured.

These data will be useful for the determination of which foot segment is in contact with the floor.





## 4. Methodology

### 4.1 Kinematic Analysis

#### 4.1.1 Segments Definition and Coordinate Systems

In order to reconstruct bones segments, markers' positions are very important. The segments' definition and markers' positions were established based on Dr. J.L Besse (an orthopedic surgeon, specialist in ankle and foot, exercising at Lyon Sud CHU) recommendations. The marker positions on the foot were defined in order to make sense for eventual comparison with pathologic subjects.

We defined a mixed model between Heidelberg model [Simon et al., 2006] and Oxford model [Carson et al., 2001], corresponding to a compromise between our needs and means.

The position of each marker is illustrated in Figure 3.7 of section 3.2.1.

The model is composed of 15 segments represented in Figure 4.1. Their name, numbering and the markers used for their definitions are clarified in Table 4.1.

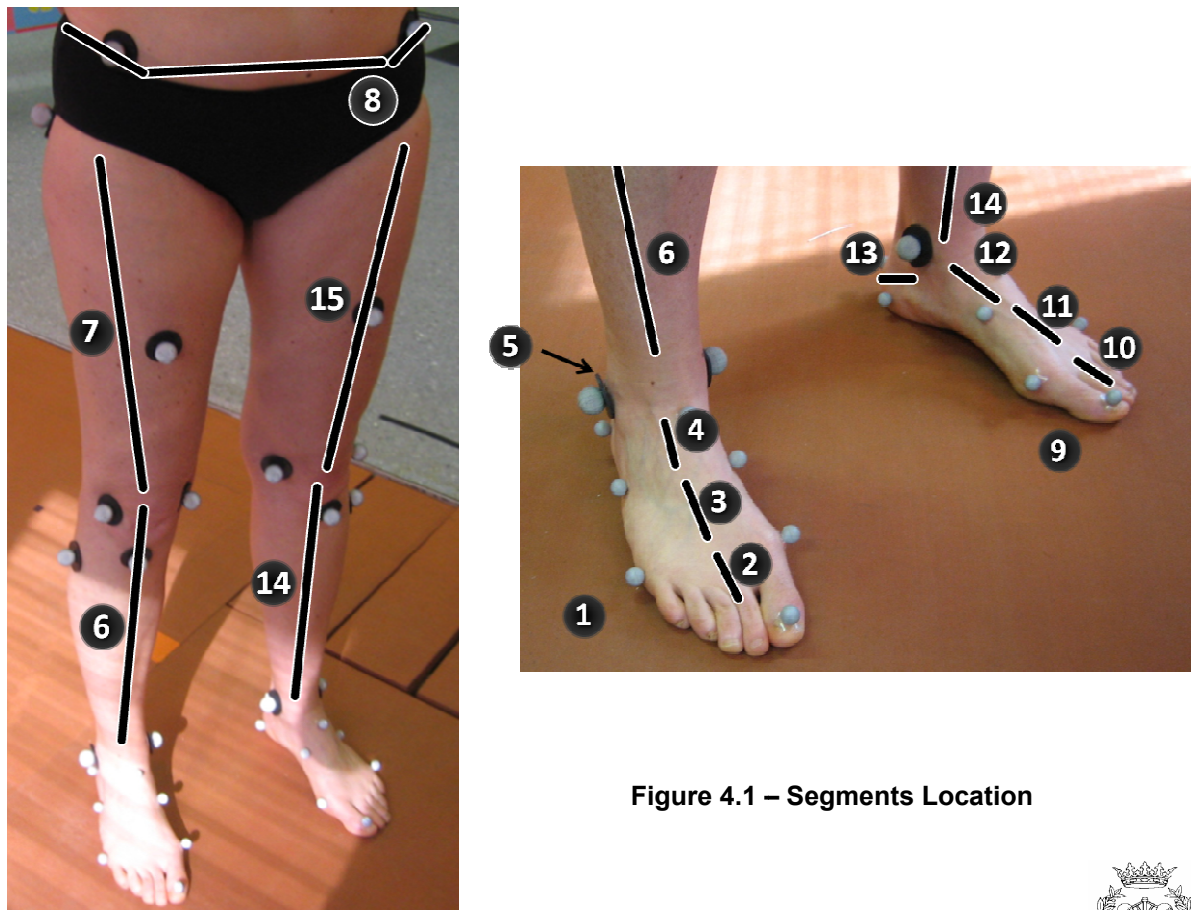


Figure 4.1 – Segments Location



Segment Name		Segment Number	Markers included in the segment
Pelvis		8	ASIS_R, ASIS_L, PSIS_R, PSIS_L
Thigh	Right Side	7	GT_R, Thigh_R, Cond_E_R, Cond_I_R
	Left Side	15	GT_L, Thigh_L, Cond_E_L, Cond_I_L
Leg	Right Side	6	TTA_R, Fibula_R Mal_E_R, Mal_I_R
	Left Side	14	TTA_L, Fibula_L, Mal_E_L, Mal_I_L
HF	Right Side	5	Calca_P_R, Calca_E_R, Calca_I_R
	Left Side	13	Calca_P_L, Calca_E_L, Calca_I_L
MF	Right Side	4	Calca_E_R, Calca_I_R, Nav R, Meta5_Base_R, Meta1_Base_R
	Left Side	12	Calca_E_L, Calca_I_L, Nav_L, Meta5_Base_L, Meta1_Base_L
FF	Right Side	3	Meta5_Base_R, Meta1_Base_R, Meta5_Head_R, Meta1_Head_R
	Left Side	11	Meta5_Base_L, Meta1_Base_L, Meta5_Head_L, Meta1_Head_L
To	Right Side	2	Meta5_Head_R, Meta1_Head_R, Toe R
	Left Side	10	Meta5_Head_L, Meta1_Head_L, Toe L
NB : Segments 1 and 9 are right and left forceplate respectively.			

Table 4.1 – Segment Definition

### Description of Segment Coordinate Systems

For the computation in Matlab<sup>®</sup> program, a Segment Coordinate System (SCS) has to be defined for each body segment in order to build the Joint Coordinate System. For the pelvis, thigh, leg and HF segments, the ISB recommendations were followed. More precisely, the axis  $\vec{u}$  is defined perpendicular to the segment frontal plane, roughly parallel to the gait axis, axis  $\vec{w}$  corresponds to the medial-lateral axis (i.e., flexion axis) and axis  $\vec{v}$  corresponds to the segment longitudinal axis.





For the three other foot segments (i.e., MF, FF, Toes), it is compulsory to define local SCS with more anatomical signification. Then, for these segments, axis  $\vec{v}$  is defined parallel to the gait axis, axis  $\vec{w}$  corresponds with the flexion axis and  $\vec{u}$  is more or less vertical pointing upward. This specificity allows the definition of foot JCS more representative of the foot movements. The axes location is represented just below and the definition, with markers location, is explained in Appendix A.3.

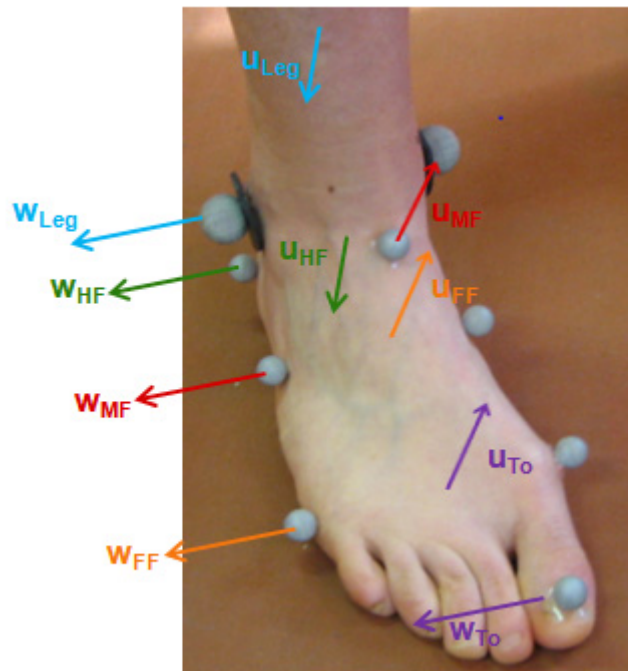


Figure 4.2 – Leg and Foot SCS

#### 4.1.2 Angular Rotation Calculation

The angular rotations are calculated using Euler angles and the Joint Coordinate System (JCS) method (also known as the method of Grood and Suntay, 1983). The latter method is widely used in biomechanical analyses. This method allows describing the orientation of a rigid body in a three-dimensional Euclidean space. The orientation is defined by composition of three rotations around three axes called “Euler axes”. When the orientation of a distal segment relative to a proximal adjacent segment is described, the first axis is linked with the proximal segment, and the third with the distal one. The second axis, called “floating axis”, is obtained as the cross product of the third and the first axes. Hence, the second axis is orthogonal to the other two, whereas the first and the third axes are not necessarily orthogonal between them.



### Euler sequences

The term Euler sequence defines the order in which the angles are calculated. In the present study, two kinds of Euler sequences are used, in order to have a more anatomic reliability. The ZXY sequence was used for four joints (FF/MF, MF/HF, Knee and Hip) and the ZYX sequence for the two other joints (To/FF and Ankle). For the ZXY sequence, the priority is given to flexion-extension and rotation movements (the abduction-adduction corresponding to the floating axis) while for the ZYX sequence, the priority is given to flexion-extension and abduction-adduction movements.

The 3 elementary rotations for sequence ZXY can be represented as in Figure 4.3:

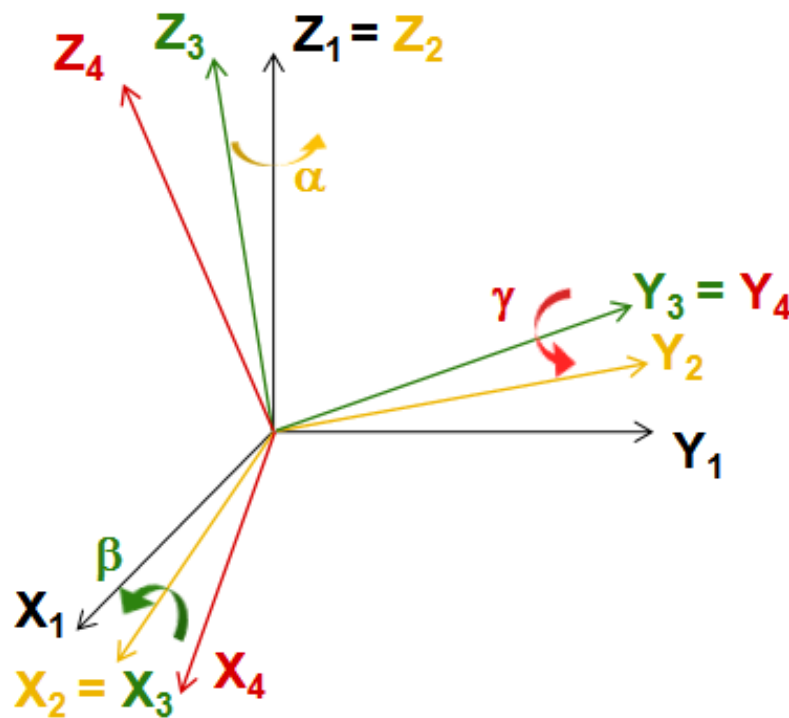


Figure 4.3 – Euler Axes



For example, with the knee, Euler axes are defined as represented in Figure 4.4:

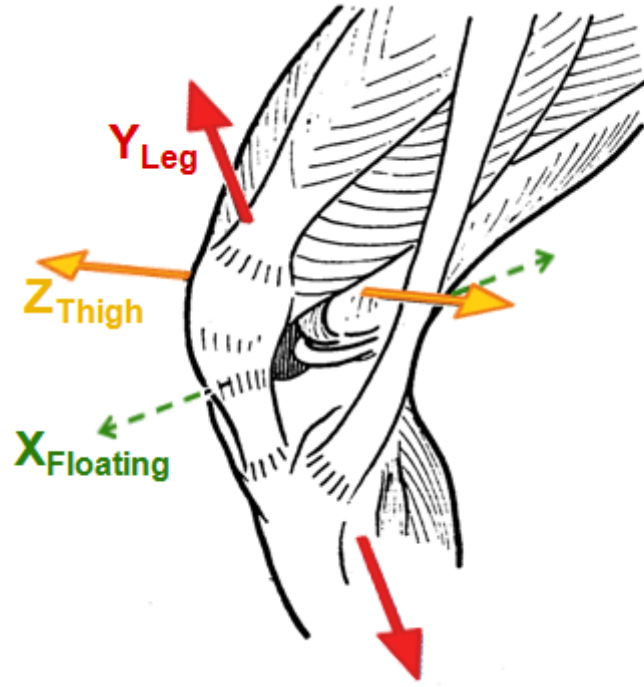


Figure 4.4 - Knee Euler Axes

The rotation matrix between the Leg and Tibia ( ${}^T_L R$ ) is the result of the multiplication of the three elementary rotations (Eq. 4.1):

$${}^T_L R = \begin{bmatrix} \cos \alpha & -\sin \alpha & 0 \\ \sin \alpha & \cos \alpha & 0 \\ 0 & 0 & 1 \end{bmatrix} \begin{bmatrix} 1 & 0 & 0 \\ 0 & \cos \beta & -\sin \beta \\ 0 & \sin \beta & \cos \beta \end{bmatrix} \begin{bmatrix} \cos \gamma & 0 & \sin \gamma \\ 0 & 1 & 0 \\ -\sin \gamma & 0 & \cos \gamma \end{bmatrix} = [\delta_{ij}] \quad \text{Eq.4.1}$$

$${}^T_L R = \begin{bmatrix} \cos \alpha \cdot \cos \gamma - \sin \alpha \cdot \sin \beta \cdot \sin \gamma & -\sin \alpha \cdot \cos \beta & \cos \alpha \cdot \sin \gamma + \sin \alpha \cdot \sin \beta \cdot \cos \gamma \\ \sin \alpha \cdot \cos \gamma + \cos \alpha \cdot \sin \beta \cdot \sin \gamma & \cos \alpha \cdot \cos \beta & \sin \alpha \cdot \sin \gamma - \cos \alpha \cdot \sin \beta \cdot \cos \gamma \\ -\cos \beta \cdot \sin \gamma & \sin \beta & \cos \beta \cdot \cos \gamma \end{bmatrix}$$

Then, the 3 angles  $\alpha$  (Flexion),  $\beta$  (Abduction) and  $\gamma$  (Rotation) are derived by:

$$\alpha = \tan^{-1} \left( \frac{-\delta_{12}}{\delta_{22}} \right) \quad \gamma = \tan^{-1} \left( \frac{-\delta_{31}}{\delta_{33}} \right) \quad \beta = \sin^{-1} (\delta_{32}) \quad \text{Eq.4.2}$$

The matrices used for the sequence ZYX are from Chèze et al. (2009) are detailed in Appendix A.5.



## 4.2 Dynamic Analysis

### 4.2.1 Inverse Dynamics

Inverse dynamics is a method for computing intersegmental forces and torques based on kinematics of a body, the body's inertial properties and the external mechanical actions on the body. It consists of considering, into a link-segment model, each body segment separately, beginning with the terminal one, in which external mechanical actions are known except the intersegmental actions. With application of the Fundamental Principle of Dynamics (FPD) (Eq. 4.3) it is possible to determine intersegmental actions applied by segment  $i+1$  on segment  $i$ .

$$\begin{cases} \sum \overrightarrow{F_{ext \rightarrow i}} \\ \sum \overrightarrow{M_{ext \rightarrow i}} \end{cases} = \begin{cases} m_i \overrightarrow{\gamma_i} \\ \overrightarrow{\delta_i} \end{cases} \quad \text{Eq. 4.3}$$

Where: -  $\sum \overrightarrow{F_{ext \rightarrow i}}$  is the sum of external forces applied on segment  $i$

-  $\sum \overrightarrow{M_{ext \rightarrow i}}$  is the sum of external moments about the proximal joint of segment  $i$

-  $m_i$  is the mass of the segment  $i$

-  $\overrightarrow{\gamma_i}$  is the acceleration of the segment  $i$  CoM

-  $\overrightarrow{\delta_i}$  is the vector that includes the time derivative of the kinetic momentum about the proximal joint and the term depending on its acceleration.

The external actions on distal segment  $i$  are: its weight  $P = mg$  (known data), the ground reaction (forceplates data), and the action of segment  $i+1$  (unique unknown)

Then, the action reaction principle (Eq. 4.4) is considered in order to know the mechanical actions of segment  $i$  on segment  $i+1$ .

$$\begin{cases} \overrightarrow{F_{i \rightarrow i+1}} \\ \overrightarrow{M_{i \rightarrow i+1}} \end{cases} = - \begin{cases} \overrightarrow{F_{i+1 \rightarrow i}} \\ \overrightarrow{M_{i+1 \rightarrow i}} \end{cases} \quad \text{Eq. 4.4}$$

That allows knowing all the mechanical actions on segment  $i+1$  except for intersegmental actions between segment  $i+2$  and  $i+1$ . By this iterative way, it is possible to determine all



intersegmental actions (due to joint constraints and musculo-tendon actions), applying alternatively FPD and action reaction principle.

The inverse dynamics approach can be illustrated by Figure 4.5:

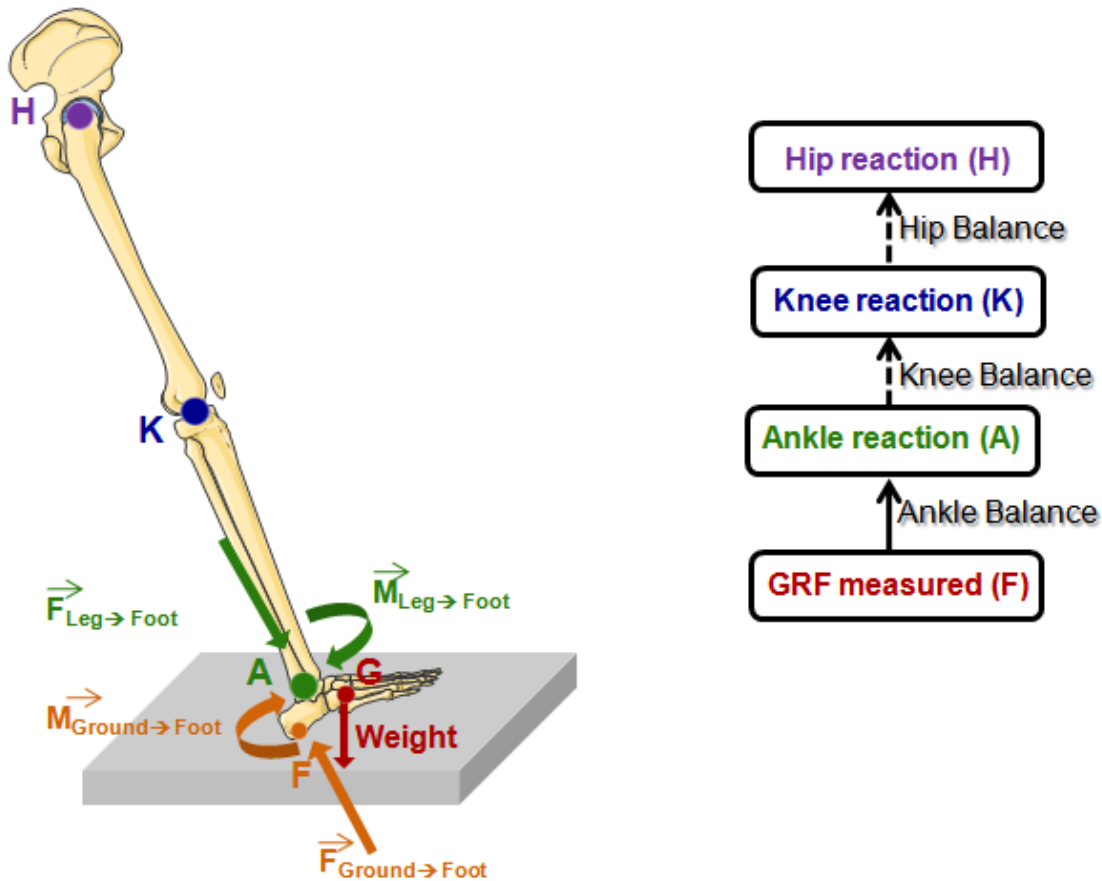


**Figure 4.5 – Inverse Dynamics Approach**

This method requires assuming the following hypotheses:

- The position of the CoM is fixed relative to proximal and distal coordinate system during the movement
- The inertia matrix of the segment is constant during the movement
- The segment length is constant during the movement

In order to execute inverse dynamics calculation, it is necessary to know the external actions on the segment in contact with the floor. If the foot is considered as a single rigid segment, the forceplate provides directly the information. But, if the foot is considered as distinct



segments, the calculation approach is more complex. This approach is detailed in the following part.

#### 4.2.2 External Actions Repartition

The external actions repartition is possible by means of baropodometric data and requires different calculation steps. This method is detailed in Samson et al. (2010) (an abstract written during the present study).

The condition of HF and MF in contact floor is considered.

#### **Data Available and Needed**

The forceplate provides globally the external actions of all the foot segments (Ff and Mf). The moment is expressed at the forceplate center, that permits calculation of the coordinates of the CoP (where the moment has non null value only on the vertical axis) and the value of this vertical moment called free torque.

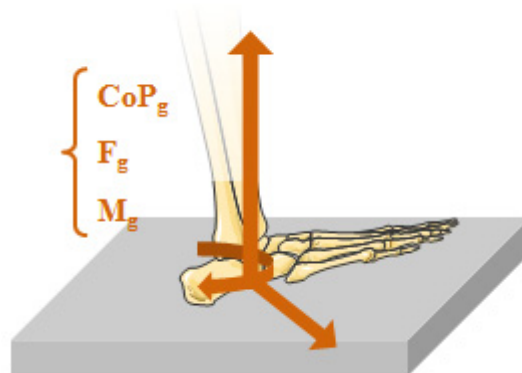


**Figure 4.6: Forceplate Data Available** (for global foot)

CoP: CoP Coordinates  
F: Ground Reaction Force  
M: Free Torque at the CoP

For the calculation of the intersegmental actions within the foot, it is compulsory to know these characteristics for each foot segment in contact with the floor.



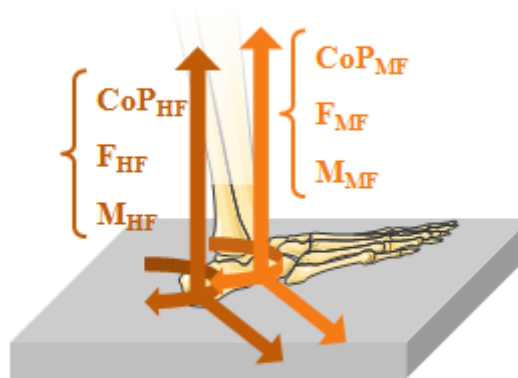


**Figure 4.7: Data Necessary** (for HF and MF in contact with the floor)

CoP: CoP Coordinates  
 F: Ground Reaction Force  
 M: Free Torque at the CoP

#### Use of baropodometric data

To share the external mechanical actions between the two segments in contact with the floor, the only available data come from the baropodometric plate which gives at each instant the plantar pressure distribution (Figure 4.8). With this, it will be possible to calculate the CoP for each segment (barycenters of pressure on the segment surface) and the ratio of vertical force applied to each segment (considering that the ratio of pressure is the same as the ratio of vertical force).

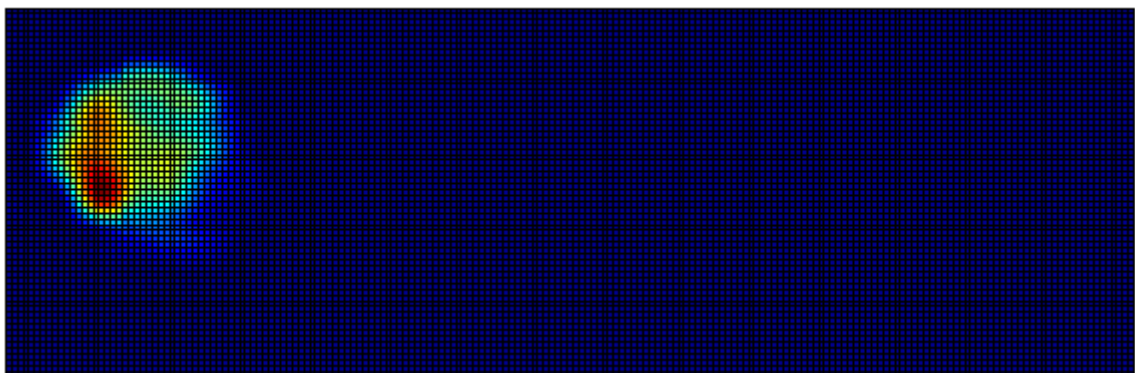


**Figure 4.8: Pressure Map** when HF and MF in floor contact

It is necessary to identify which sensor corresponds to which foot segment.



The cutting of global plantar pressure map is realized using the marker coordinates during flat foot contact. That yields to the four masks displayed in Figure 4.9:

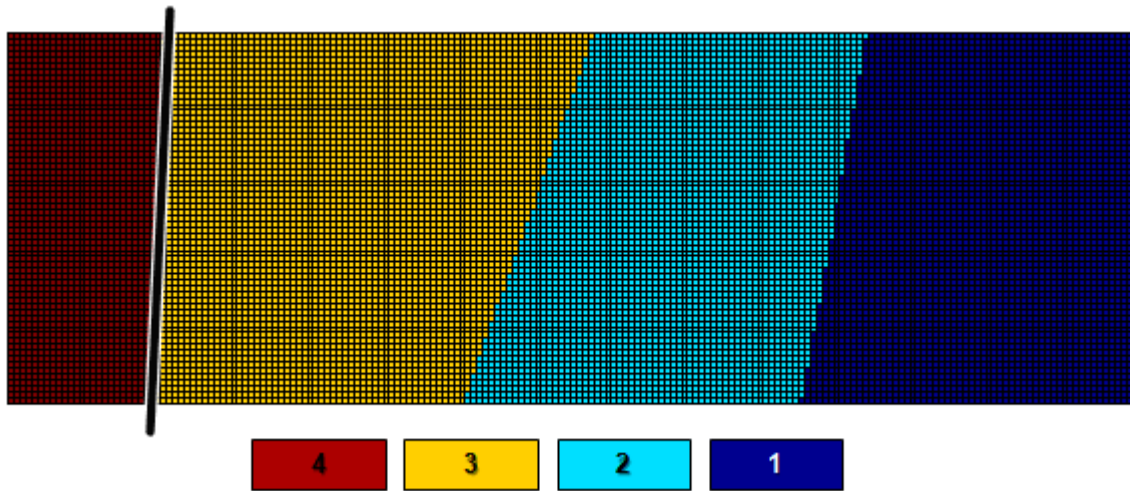


**Figure 4.9 : Masks Allocation**

The sequence of the masks activation is identified as sections numbered as it is illustrated in Figure 4.10:

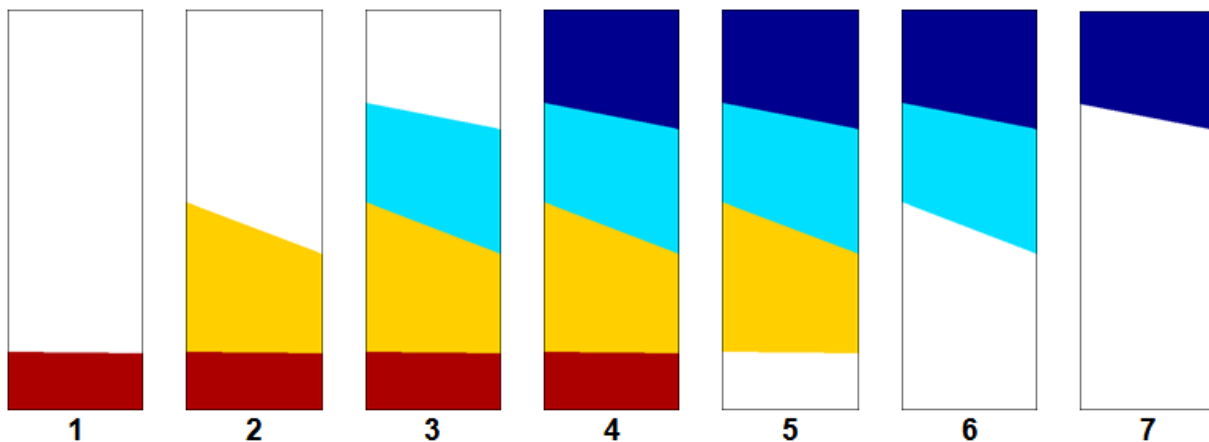


**Figure 4.10 – Section Corresponding to the Activated Masks**

With the cutting of global plantar pressure into masks, it is possible to identify for the global pressure map, the ratio of pressure on each mask at each instant.





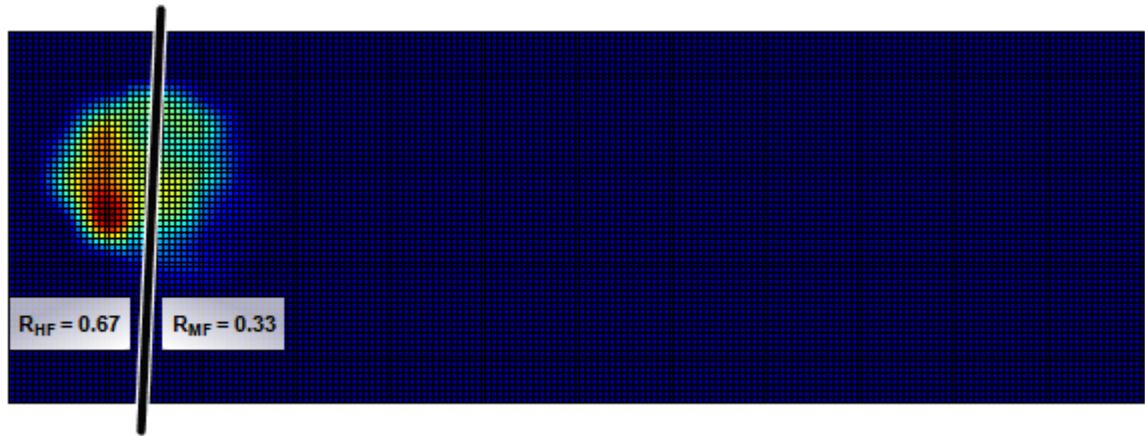


Figure 4.11 – Masks Ratio

This ratio is used in order to distribute the global vertical force  $F_y$  measured by the forceplate between HF and MF (Eq. 4.5)

$$\begin{cases} Fy_{HF} = R_{HF} \cdot Fy_g \\ Fy_{MF} = R_{MF} \cdot Fy_g \end{cases} \quad \text{Eq. 4.5}$$

Then, the CoP of each segment is calculated as the barycenter of the pressure for the corresponding mask.

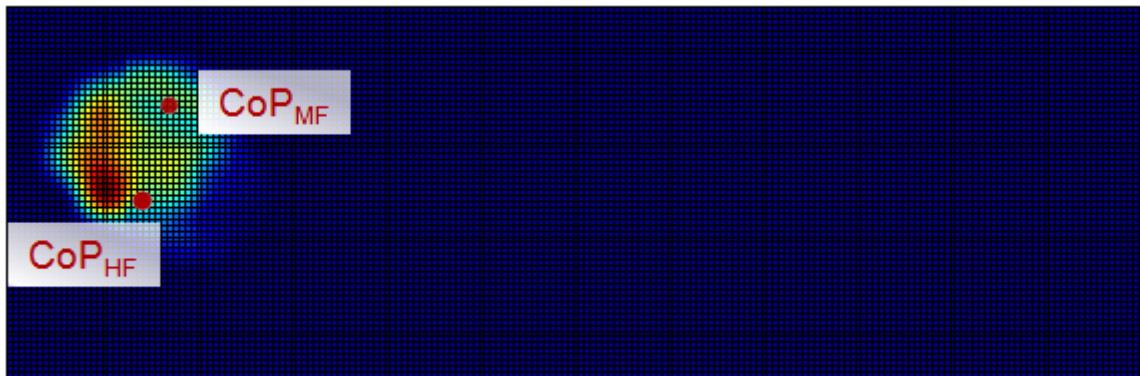


Figure 4.12 – CoP for Each Segment

### Use of Coulomb's Laws

The baropodometric plate provides information only for the normal force distribution. In order to distribute the other contact actions (tangential force and free torque), Coulomb's Laws are used considering the foot floor contact as a contact without slipping and pivoting due to dry friction. According to those, two coefficients expressing the relationship between tangential



force norm and normal force norm (tangential coefficient  $k_1$ ) and between pivoting moment norm and normal force norm (pivot resistance coefficient  $k_2$ ) are defined (Eq. 4.6).

$$k_1 = \frac{\|\vec{F}_{xz}\|}{\|\vec{F}_y\|} \quad k_2 = \frac{\|\vec{M}_y\|}{\|\vec{F}_y\|} \quad \text{Eq. 4.6}$$

These coefficients are calculated with the global forceplate data and are considered the same for each foot segment.

An additional hypothesis is necessary relative to the tangential force repartition, because Coulomb's Law application provides the resultant of tangential force (norm vector relationship) but not the repartition between axes X and Z. It is considered that the tangential action global repartition between X and Z is the same for all foot segments. The coefficients  $k_3$  and  $k_4$  (Eq. 4.7) are so calculated from the global forceplate data and then applied for each segment.

$$k_3 = \frac{\|\vec{F}_x\|}{\sqrt{\|\vec{F}_x\|^2 + \|\vec{F}_z\|^2}} \quad k_4 = \frac{\|\vec{F}_z\|}{\sqrt{\|\vec{F}_x\|^2 + \|\vec{F}_z\|^2}} \quad \text{Eq. 4.7}$$

This last hypothesis is relative to the mechanical actions directions: it is considered that the direction of external actions is the same for all foot segments.

With the previous considerations, it is possible to obtain the external actions during the different sections of stance phase (Figure 4.13)

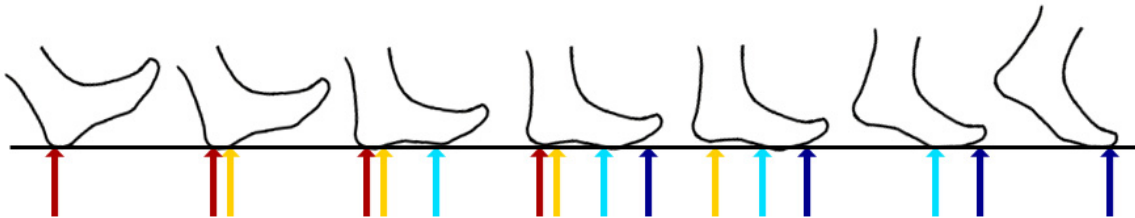


Figure 4.13 – GRF Distribution during SP



This external action repartition requires a particular attention for the moment calculation during the inverse dynamic method. Indeed, because of the force application on two distinct points, it is necessary to consider two distinct lever arms. For example, in Figure 4.14, in order to calculate the moment at the point P (FF/MF Joint) it is necessary to transport the moment from the point D (at To/FF Joint, previously computed by equilibrating the segment To) considering the distance PD and add the action of the force in B considering the lever arm PB.

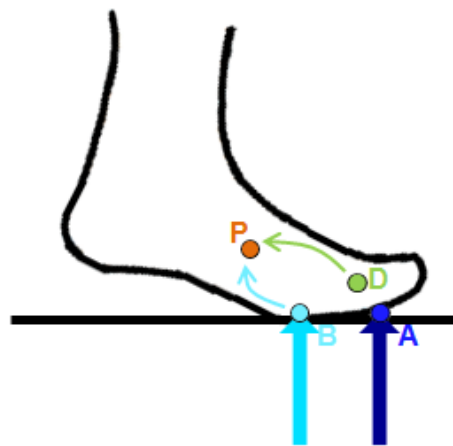


Figure 4.14 – Toe and FF in Contact with the Floor

#### 4.2.3 Body Segments Inertial Parameters

In order to compute inverse dynamics, it is necessary to use the Body Segment Inertial Parameters (BSIP) data. In the present study, the equations used were those of Dumas et al. (2007). The advantage of using these references is that “these scaling equations are directly applicable in the conventional SCS and do not restrain the position of the Center of Mass (CoM) and the orientation of the principal axes”.

The foot SCS is defined as illustrated in Figure 4.15:

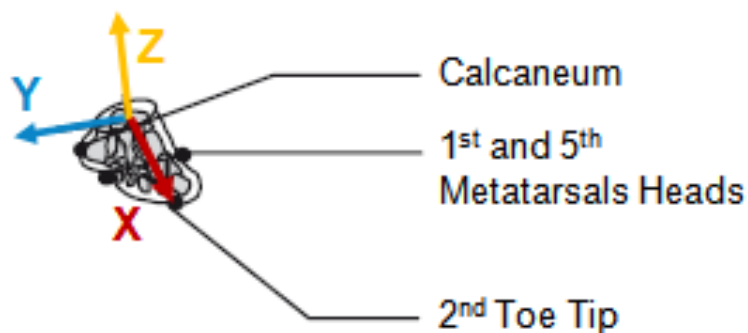


Figure 4.15 – Foot SCS (Dumas et al., 2007)



The scaling factors for the foot are:

Scaling factors for :	Mass	Position of CoM			Inertia tensor					
	m (%)	X (%)	Y (%)	Z (%)	r <sub>xx</sub> (%)	r <sub>yy</sub> (%)	r <sub>zz</sub> (%)	r <sub>xy</sub> (%)	r <sub>xz</sub> (%)	r <sub>yz</sub> (%)
Entire Foot	1	44,3	4,4	-2,5	12	25	25	7(i)	5	3(i)

Table 4.2 – Scaling Factors (Dumas et al., 2007)

(i) denotes negative product of inertia

From these factors, in the foot SCS (Figure 4.15), the position of the CoM and the complete inertia tensor are derived directly by:

$$\begin{bmatrix} 0.443 & L_{foot} \\ 0.044 & L_{foot} \\ -0.025 & L_{foot} \end{bmatrix} \text{ and } \begin{bmatrix} (0.12 L_{foot})^2 & (0.07i L_{foot})^2 & (0.05 L_{foot})^2 \\ (0.07i L_{foot})^2 & (0.25 L_{foot})^2 & (0.03i L_{foot})^2 \\ (0.05 L_{foot})^2 & (0.03i L_{foot})^2 & (0.25 L_{foot})^2 \end{bmatrix} \times 0.01m_{body} \quad \text{Eq. 4.8}$$

Where  $0.01m_{body}$  is the mass of the foot segment.

However, for the present study, coefficients for each foot segment are required. Therefore, some simplifying assumptions are necessary and the following method is developed for their calculation.

According to Table 4.2, it is possible to notice that the scaling factors relative to the position of the CoM for axes Y and Z and those relative to the inertia tensor for non-diagonal terms are negligible with respect to the other ones. Moreover, the coefficients corresponding to the inertia moments about Y and Z axes are equal.

These considerations yields the assumption that the foot can be modeled as a cylinder with principal axis X, i.e., nullify the negligible coefficients. Using this method, it will be easier to calculate the scaling factors for each foot segment. The approach is detailed just below.

Besides, the mass and inertia of segment Toe are ignored, because they are very small.



**Position of CoM**

The position of CoM is defined by  $\frac{X}{100} \cdot L(s)$ , this permits to conclude that the scaling factor X is proportional to the segment length. So, it will be easy to compute the factors X for each foot segment considering the length ratio  $L_s$  (Eq. 4.9)

$$L_s = \frac{L(s)}{\sum_{s=3}^{s=5} L(s)} \quad \text{Eq 4.9}$$

With: -  $L(s)$  the length of the segment s  
 -  $L_s$  : the length ratio of the segment s (relative to the length of the three foot segments HF, MF, FF)

*Notice that the segment Toe does not appear in the length ratio.*

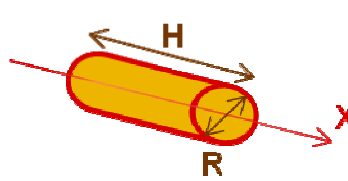
The scaling coefficient X for a segment s can be expressed as (Eq. 4.10):

$$X(s) = L_s \cdot X \quad \text{Eq 4.10}$$

**Inertia tensor**

Considering the negligible values of the non diagonal terms of the inertia matrix, it is possible to represent the foot as a cylinder with X as the principal axis.

The inertia matrix of a cylinder with mass M, radius R and length H is:



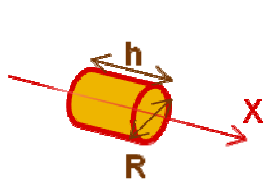
The diagram shows a yellow cylinder with a red outline. A double-headed arrow above the cylinder indicates its length H. A double-headed arrow across the circular face indicates its radius R. A red arrow labeled X points along the longitudinal axis of the cylinder, representing the principal axis.

$$J = \begin{bmatrix} \frac{1}{2}MR^2 & 0 & 0 \\ 0 & \frac{1}{4}MR^2 + \frac{1}{12}MH^2 & 0 \\ 0 & 0 & \frac{1}{4}MR^2 + \frac{1}{12}MH^2 \end{bmatrix} \quad \text{Eq 4.11}$$

Thus, the scaling factors for inertia tensor are not directly proportional to the cylinder length. In order to establish the relationship between these coefficients for all foot segments and each foot segment the segment foot is considered as a cylinder with mass m, radius R and length h.



The inertia matrix of this cylinder is:



$$J = \begin{bmatrix} \frac{1}{2}mR^2 & 0 & 0 \\ 0 & \frac{1}{4}mR^2 + \frac{1}{12}mh^2 & 0 \\ 0 & 0 & \frac{1}{4}mR^2 + \frac{1}{12}mh^2 \end{bmatrix} \quad \text{Eq 4.12}$$

Considering that  $m=L_sM$  and  $h = L_sH$ , it is possible to express the coefficient relative to the inertia tensor for each segment  $((I_{xx})_s, (I_{yy})_s$  and  $(I_{zz})_s$ ) as a function of the coefficients for all foot segments  $(I_{xx}, I_{yy}$  and  $I_{zz})$  :

$$\begin{cases} (r_{xx})_s = L_s \cdot r_{xx} \\ (r_{yy})_s = (r_{zz})_s = \frac{1}{2}(r_{xx})_s + L_s^3 (r_{yy} - \frac{1}{2}r_{xx}) \end{cases} \quad \text{Eq 4.13}$$

Those relations allow computing the coefficients of BSIP for each subject. An example of results, for the subject 1 is in Table 4.3:

Scaling factors for :	Mass	Position of CoM			Inertia tensor					
	m (%)	X (%)	Y (%)	Z (%)	$r_{xx}$ (%)	$r_{yy}$ (%)	$r_{zz}$ (%)	$r_{xy}$ (%)	$r_{xz}$ (%)	$r_{yz}$ (%)
Ground	0	0	0	0	0	0	0	0	0	0
Hallux	0	0	0	0	0	0	0	0	0	0
ForeFoot	0,26	11,34	0	0	3,07	1,85	1,85	0	0	0
MiddleFoot	0,55	24,54	0	0	6,65	6,55	6,55	0	0	0
HindFoot	0,19	8,42	0	0	2,28	1,27	1,27	0	0	0
Leg	4,5	-4,8	-41	0,7	28	10	28	0	0	0
Thigh	14,6	-7,7	-37,7	0,9	31	19	32	0	0	0
Pelvis	14,6	-0,9	-23,2	0,2	91	100	79	0	0	0

Table 4.3 – Subject 1 BSIP

It is important to notice that parameters are different for males and females, and because the study includes both, two separate tables were used. The reference tables are exposed in Appendix A.5.



## 5. Results and discussion

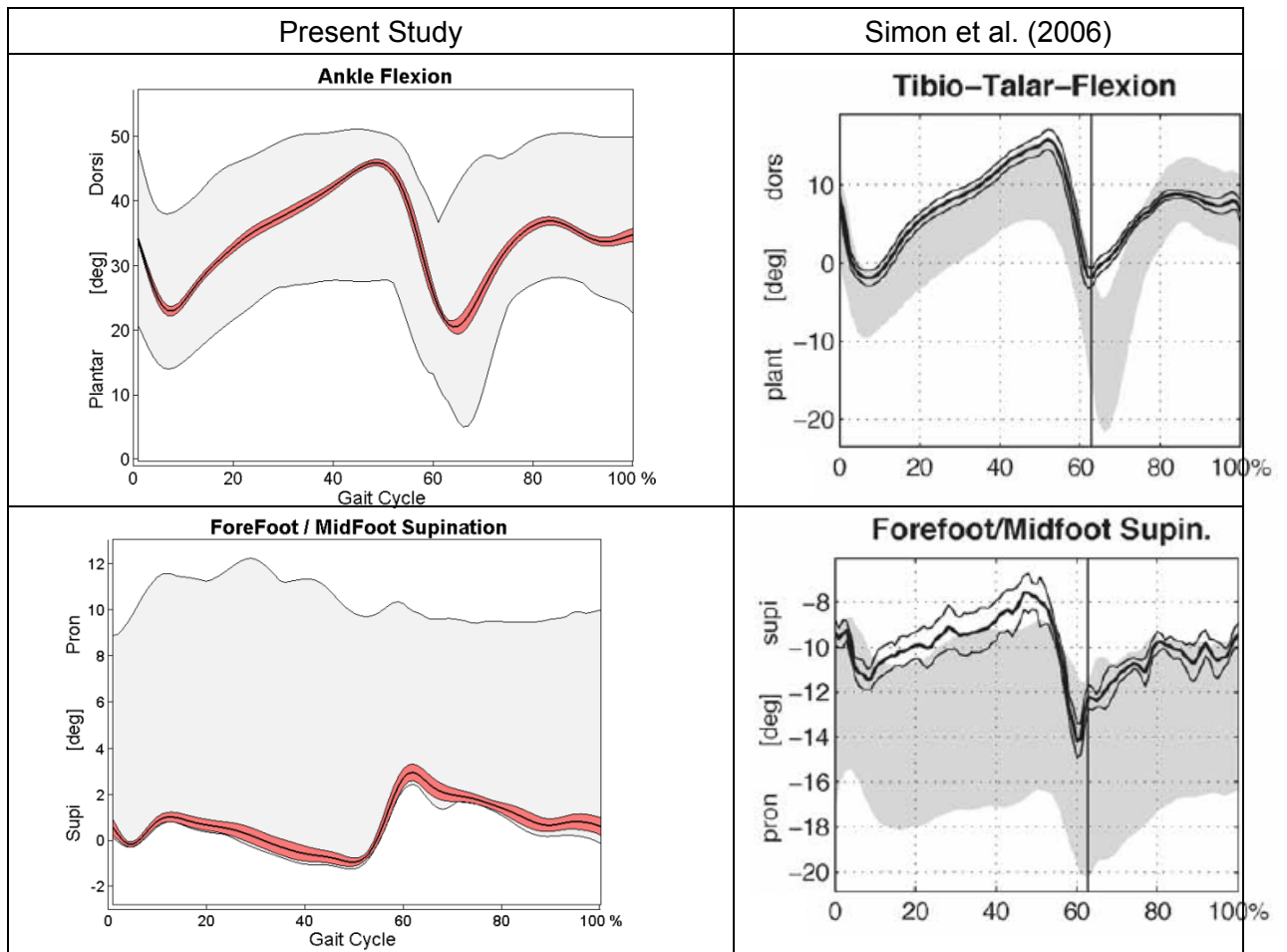
### 5.1 Kinematics

Different kinematic results can be obtained. It was chosen to expose some of them in order to compare with the literature. Moreover, some characteristic angles are exposed.

#### 5.1.1 Literature Comparison

The study compared is Simon et al. (2006) because kinematics is observed during a whole gait cycle, such as it is done in the present study.

The ankle flexion, FF-MF supination, To-FF flexion and To-FF abduction are:



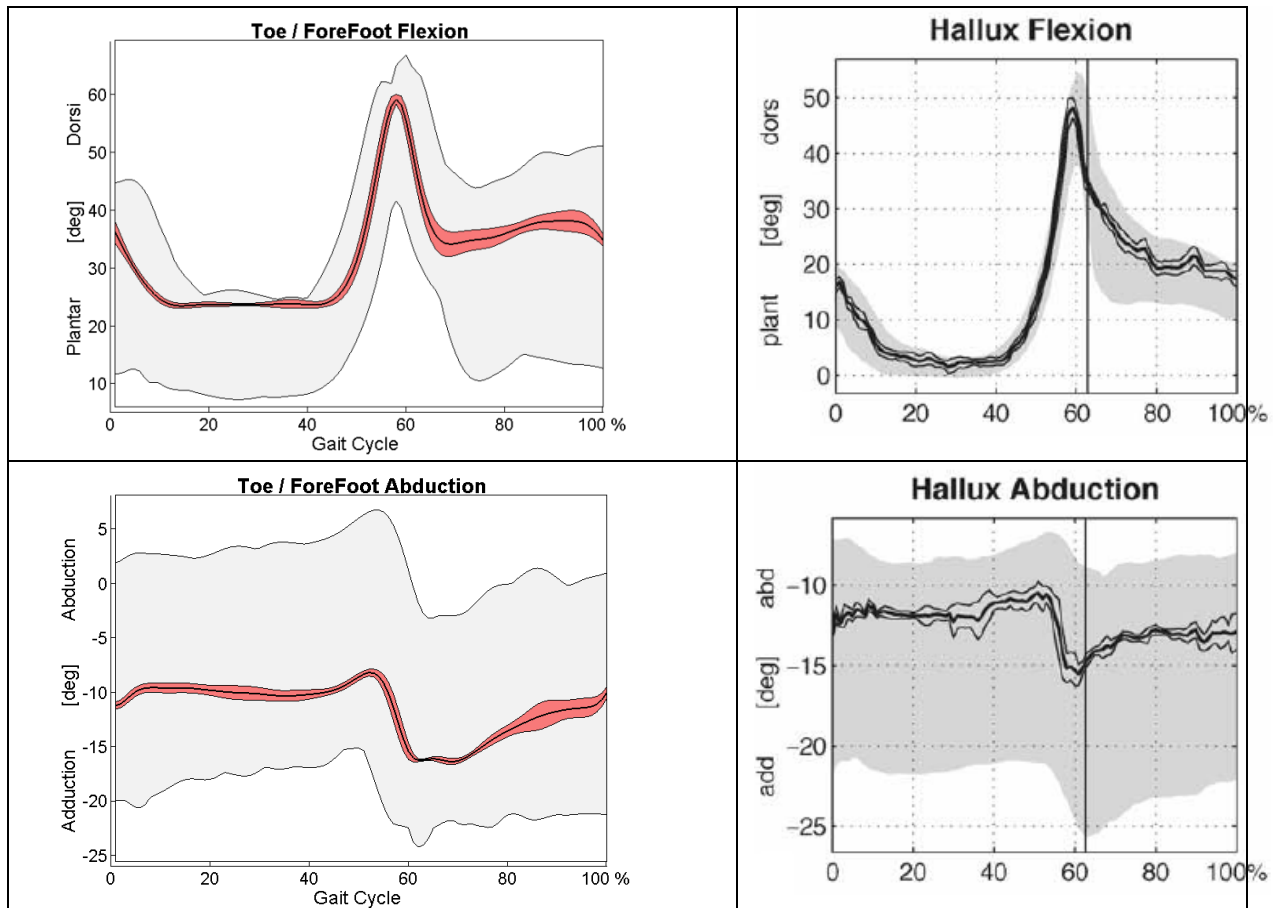


**Figure 5.1 – Kinematic Comparison**

Foot and ankle kinematics normalized to the gait cycle.

*Heavy lines represent mean values for five right strides of a given subject (eight for literature data)  
 Red zones (or thin lines for literature data) present one standard deviation.  
 Grey zones present the range for the 10 participants combined.*

The similarities between the present study and Simon et al. (2006) results are clear. Both pattern and RoM are consistent. The pronation / supination curve is opposed because in the present study convention, pronation is positive while in the literature is the supination positive. The intra-subject variability (red zone) is acceptable while the large range of all the participants (grey zone) show the important inter-subject variability.

Besides, it is important to notice that zero values are not similar in the two studies: a gap between the curves can be observed. Indeed, the choice of the reference position (zero definition) is a recurrent problem for results comparison.

The supplementary similarities with Myers et al. (2004) graphs allow the validation of the present foot modeling, as far as the kinematics is concerned.





### 5.1.2 Present Study Contribution

Additionally, the present foot model provides some other different angles:

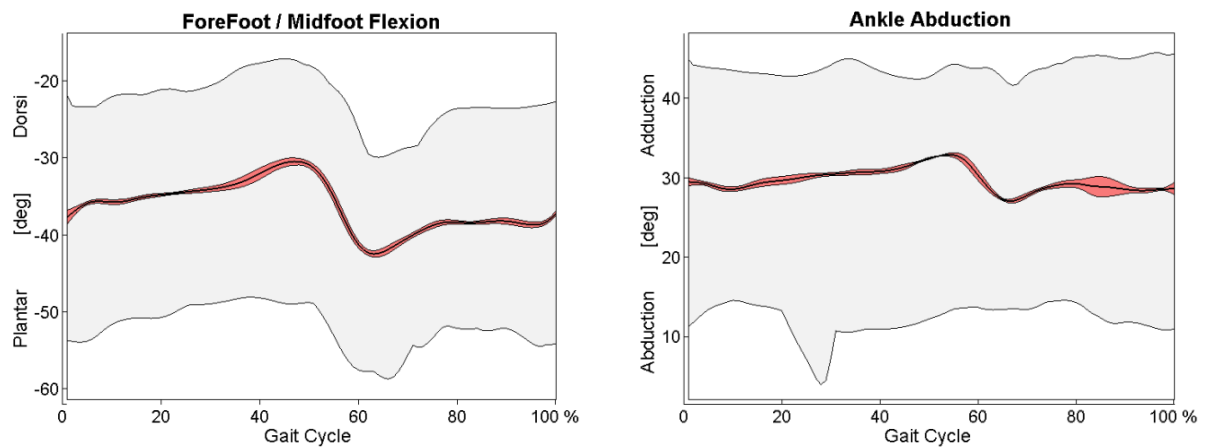


**Figure 5.2 – Additional Angles**

*The drawing convention is the same as Figure 5.1*

Those angles were chosen because of their RoM quite important and their intra-subject repeatability.

### 5.2 Measurement Repeatability

In order to check the repeatability of the SP duration and sections sequence, the GRF of the ten trials is observed for one subject.

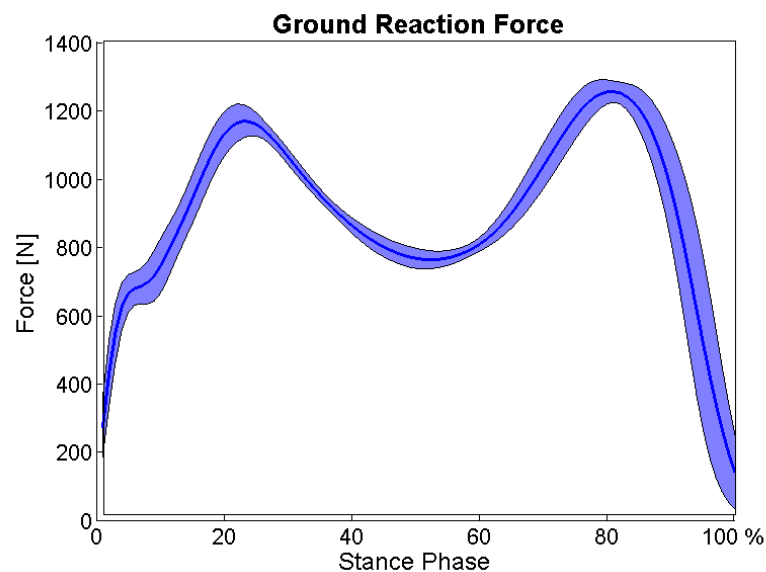


**Figure 5.3 – Ground Reaction Force**



The standard deviation is acceptable, that confirms the SP repeatability. This check is essential for the validation of the use of a unique baropodometric dynamic roll off for the external actions repartition in all the trials on forceplate.

### 5.3 External Actions Distribution

The repartition of external actions on each mask obtained from baropodometric data (Forces on the axis X, Y and Z and Free Torque) during a SP is represented on the following figures.

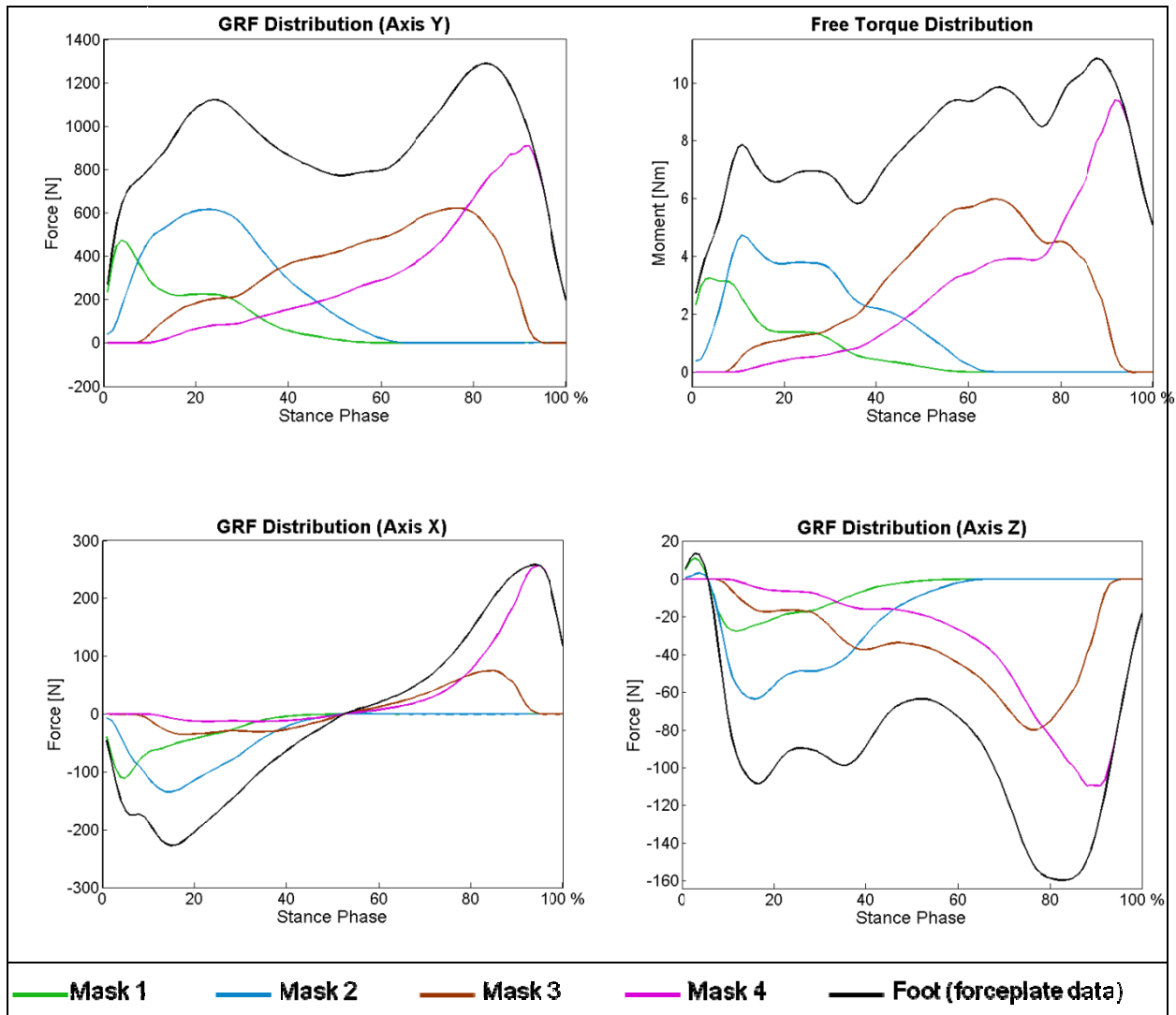


Figure 5.4 – External Actions Distribution

These graphs show that the sum of external actions on each segment is really the value of the external actions on the global foot.

Nevertheless, it is important to notice that the mask cutting has been obtained by marker projection on the floor during the flat foot contact, in order to define the foot shape. Actually,

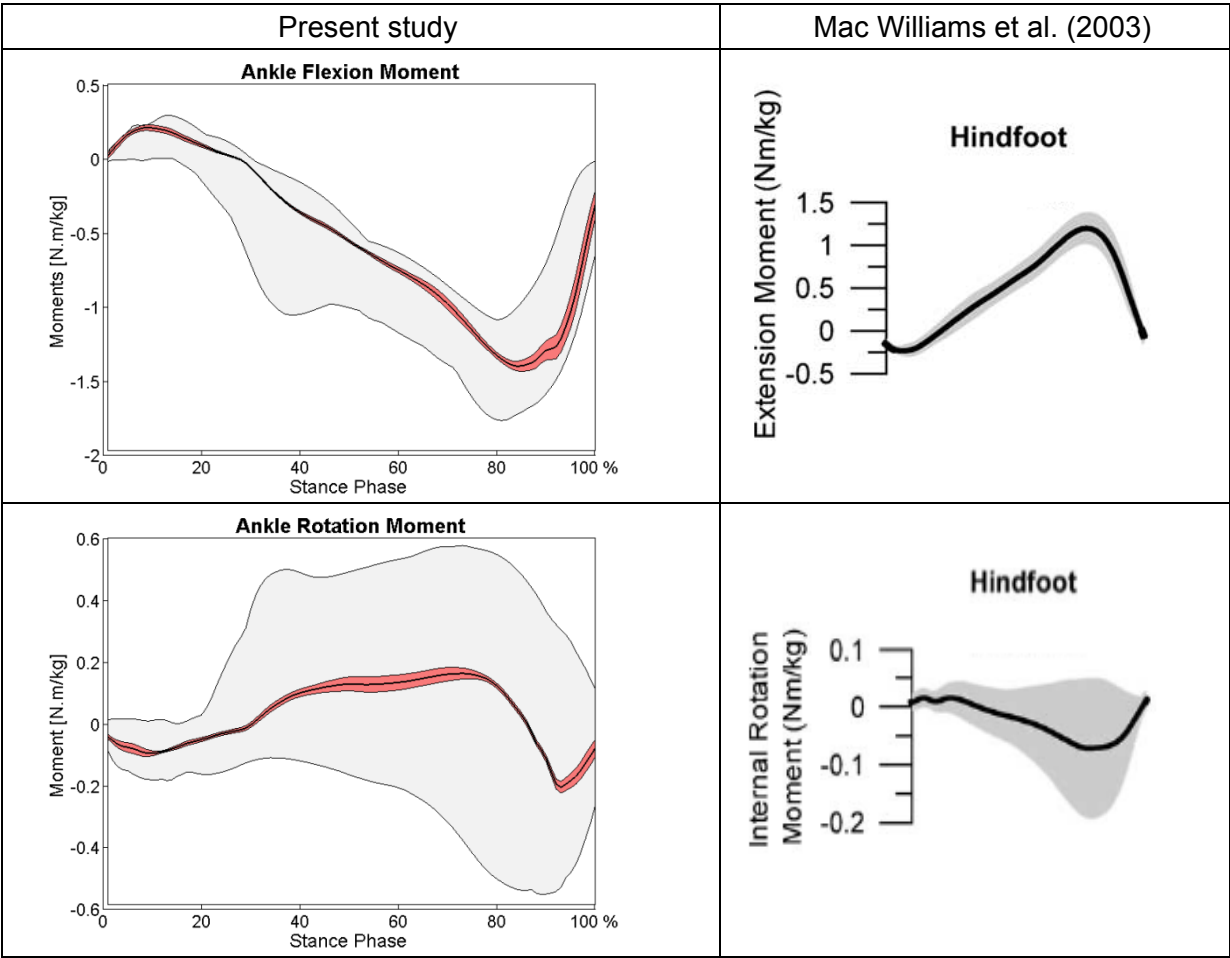


the surface shape obtained by this way is smaller than the real plantar pressure map. Because this surface shape is used in order to determine line separation, it can be admitted a small influence of this error.

5.4 Dynamics

5.4.1 Literature Comparison

The results obtained in the present study are compared with those of Mac Williams et al. (2003), as these authors are the only ones who propose a distribution of the GRF on the different foot segments in order to compute the foot joint moments.



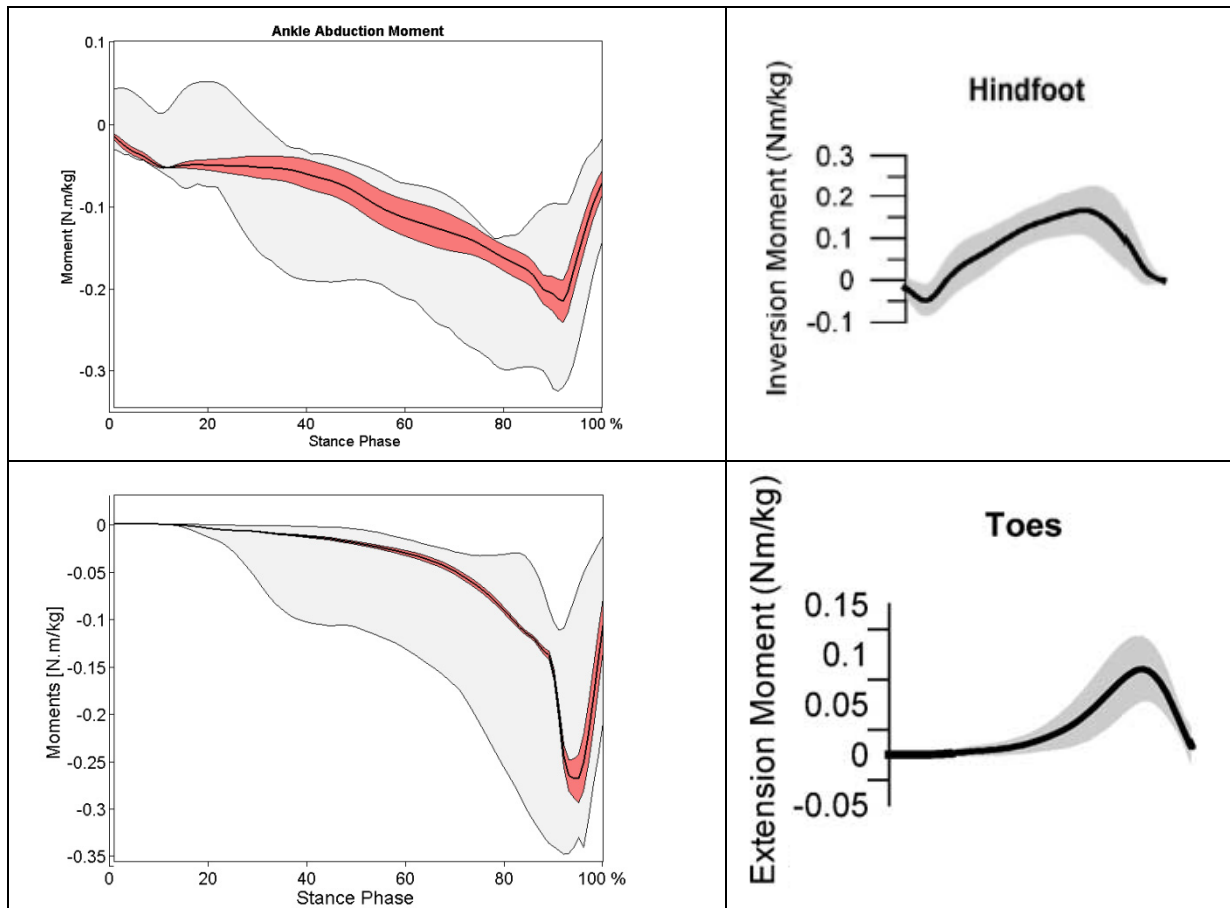


**Figure 5.5 – Dynamic Comparison**

Joint moments are normalized to subject body mass  
*The drawing convention is the same as in Figure 5.1*

In the present study, the joint actions from proximal to distal segment are displayed while Mac Williams et al. (2003) compute external moments, therefore the graphs are reversed. Nevertheless, the pattern and the RoM are similar in both studies. Besides, considering only present study ankle rotation moment, the variability seems to be strangely high, but literature graph is similar.



### 5.4.2 Present Study Contribution

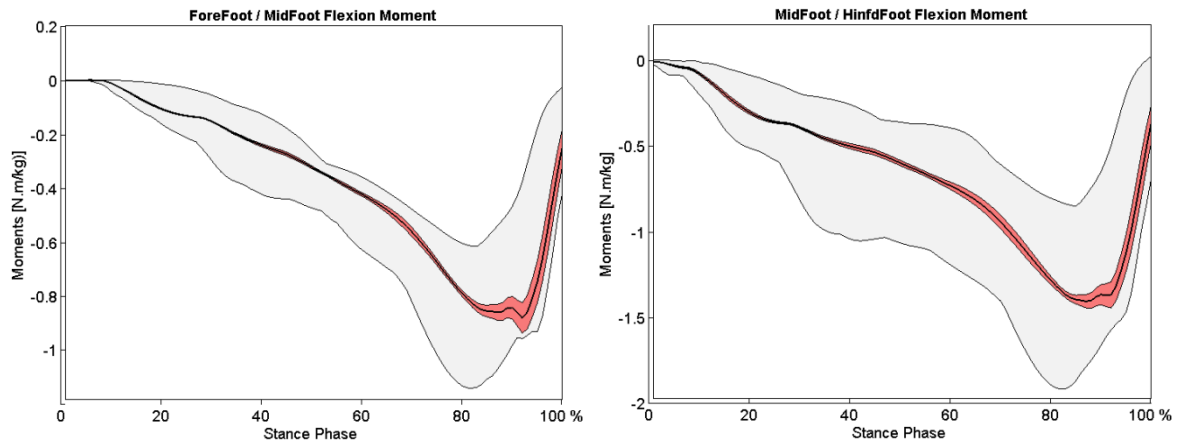


**Figure 5.5 – Additional Moments**

Joint moments are normalized to subject body mass  
*The drawing convention is the same as in Figure 5.1*

These additional graphs provide a better knowing of joint flexion moments within the foot. The high variability of the moment parameters is underlined.

The consistency of our results with those displayed in published studies allows the evaluation of the present foot model. Moreover, because it is a model, some study limits have to be considered. The lack of reference position in order to define zero value for angles leads to a more difficult comparison with literature data. The errors introduced by using a non invasive protocol (skin markers) and baropodometric data have to be also thought about. Finally, the high inter-subject variability, considering yet asymptomatic subjects, requires future studies including more subjects in order to be able to realize statistical analysis and facilitate the pathologic case detection.





## Conclusions

---

In the present study, a multi-segment foot model has been proposed to assess movements and mechanical actions within the foot. The link between kinematics and dynamics has been done using baropodometric data in order to distribute vertical ground reaction force. The distribution of transversal force and free torque has been processed considering a recent approach [Samson et al., 2010] different from the literature [Mac Williams et al., 2003]. This original method was developed during the present study. Kinematic and dynamic results have similarities with literature that confirms the reliability of the proposed model.

This model could have different fields of application: in the clinical field to study the foot biomechanics of pathologic patients, in orthopedics to design ankle orthoses and prostheses and in the design of more ergonomic shoes.

Future baropodometric studies considering the different sections duration, their repartition and their repeatability during stance phase would be necessary to characterize more precisely the stance phase.

Future works, involving more subjects, will lead to make the pathologic case detection possible.







# Acknowledgements

---

This work couldn't have been achieved without the implication and the participation of many people I would like to thank.

Special thanks go to my French supervisor **Pr. L. Chèze** who offered me the opportunity to work on this specially assigned research subject. Her expansive knowledge and priceless experience as well as her helpful advices have been decisive for this study success. A special credit has to be given to my Spanish supervisor **Dr. J.M. Font Llagunes** who has been present in spite of the distance and who offers me the possibility to continue our collaboration with a joint supervision thesis.

I also would like to thank **Dr R. Dumas** for his useful advice and his availability. Thanks to **Dr J.L. Besse** for having shared a piece of anatomical advice and letting me assist to an ankle prosthesis surgical intervention.

Thanks to **W. Samson** for the collaboration work done and his help for the experimental training. It was a very good first experience for me to write an abstract accepted in a national conference during my graduation project.

Finally, thanks to all the people who have contributed to the redaction of this English version report.





# Bibliography

---

## References in the Text

### Articles

ARNDT, A., WOLF, P., LIU, A., NESTER, C., STACOFF, A., JONES, R., LUNDGREN, P., LUNDBERG, A. *Intrinsic foot kinematics measured in vivo during the stance phase of slow running*. Journal of Biomechanics, Vol. 40(12), 2007, p. 2672-2678.

CARSON, M.C., HARRINGTON, M.E., THOMPSON, N., O'CONNOR, J.J., THEOLOGIS, T.N. *Kinematic analysis of a multi-segment foot model for research and clinical applications: a repeatability analysis*. Journal of Biomechanics, Vol. 34(10), 2001, p. 1299-307.

CHEZE, L., FREGLY, B.J., DIMNET, J. *A solidification procedure to facilitate kinematic analyses based on video system data*. Journal of Biomechanics, Vol. 28(7), 1995, p. 879-884.

CHEZE, L., DUMAS, R., COMTET, J.J., RUMELHART, C., FAYET, M. *A joint coordinate system proposal for the study of the trapeziometacarpal joint kinematics*. Computer Methods in Biomechanics and Biomedical Engineering, Vol. 12(3), 2009 Jun, p. 277-282.

CHIARI, L., DELLA CROCE, U., LEARDINI, A., CAPPOZZO, A. *Human movement analysis using stereophotogrammetry. Part 2: Instrumental Errors*. Gait and Posture, Vol. 21(2), 2005, p. 197-21

DUMAS, R., CHEZE, L., VERRIEST, J.P. *Adjustments to McConville et al. and Young et al. body segment inertial parameters*. Journal of Biomechanics, Vol. 40(3), 2007, p. 542-553.

EHRIG, R.M., TAYLOR, W.R., DUDA, G.N., HELLER, M.O. *A survey of formal methods for determining the centre of rotation of ball joints*. Journal of Biomechanics, Vol. 39(15), 2006, p. 2798-2809.

GORTON, G.E. 3<sup>rd</sup>, HEBERT, D.A., GANNOTTI, M.E. *Assessment of the kinematic variability among 12 motion analysis laboratories*. Gait & Posture, Vol. 29(3) 2009 Apr, p. 398-402.

GROOD, E.S., SUNTAY, W.J. *A joint coordinate system for the clinical description of three-dimensional motions: Application to the knee*. Journal of Biomechanical Engineering, Vol. 105(2), 1983, p 136-144.

HOUCK, J.R., TOME, J.M., NAWOCZENSKI, D.A. *Subtalar neutral position as an offset for a kinematic model of the foot during walking*. Gait & Posture, Vol. 28(1), 2008 Jul, p. 29-37.



HUNT, A.E., SMITH, R.M., TORODE, M., KEENAN, A.M. *Inter-segment foot motion and ground reaction forces over the stance phase of walking*. Clinical Biomechanics (Bristol, Avon), Vol. 16(7), 2001 Aug, p. 592-600.

INGROSSO, S., BENEDETTI, M.G., LEARDINI, A., CASANELLI, S., SFORZA, T., GIANNINI, S. *GAIT analysis in patients operated with a novel total ankle prosthesis*. Gait & Posture, Vol. 30(2), 2009, p. 132-137.

JENKYN, T.R., NICOL, A.C. *A multi-segment kinematic model of the foot with a novel definition of forefoot motion for use in clinical gait analysis during walking*. Journal of Biomechanics, Vol. 40 (14), 2007, p. 3271-3278.

KADABA, M.P., RARNAKRISHNAN, H.K., WOOTEN, M.E., GAINEY, J., GORTON, G., COCHRAN, G.V.B. *Repeatability of kinematic, kinetic, and electromyographic data in normal adult gait*. Journal of Orthopaedic Research, Vol. 7(6), 1986, p. 849-860.

KEPPLE, T.M., STANHOPE, S.J., LOHMANN, K.N., ROMAN, N.L. *A video-based technique for measuring ankle-subtalar motion during stance*. Journal of Biomedical Engineering, Vol. 12(4), 1990 Jul, p.273-280.

LEARDINI, A., BENEDETTI, M.G., CATANI, F., SIMONCINI, L., GIANNINI, S. *An anatomically based protocol for the description of foot segment kinematics during gait*. Clinical Biomechanics (Bristol, Avon), Vol. 14 (8), 1999 Oct, p. 528-536.

LEARDINI, A., BENEDETTI, M.G., BERTI, L., BETTINELLI, D., NATIVO, R., GIANNINI, S. *Rear-foot, mid-foot and fore-foot motion during the stance phase of gait*. Gait & Posture, Vol. 25(3), 2007 Mar, p. 453-462.

LUNDGREN, P., NESTER, C., LIU, A., ARNDT, A., JONES, R., STACOFF, A., WOLF, P., LUNDBERG, A. *Invasive in vivo measurement of rear-, mid- and forefoot motion during walking*. Gait & Posture, Vol. 28(1), 2008, p. 93-100.

MAC WILLIAMS, B.A., COWLEY, M., NICHOLSON, D.E. *Foot kinematics and kinetics during adolescent gait*. Gait & Posture, Vol. 17(3), 2003 Jun, p. 214-224.

MOSELEY, L., SMITH, R., HUNT, A., GANT, R. *Three-dimensional kinematics of the rearfoot during the stance phase of walking in normal young adult males*. Clinical Biomechanics (Bristol, Avon), Vol. 11(1), 1996 Jan, p. 39-45.

MYERS, K.A., WANG, M., MARKS, R.M., HARRIS, G.F. *Validation of a multisegment foot and ankle kinematic model for pediatric gait*. IEEE transactions on neural systems and rehabilitation engineering, Vol. 12(1), 2004 Mar, p. 122-130.

NESTER, C., JONES, R.K., LIU, A., HOWARD, D., LUNDBERG, A., ARNDT, A., LUNDGREN, P., STACOFF, A., WOLF, P. *Foot kinematics during walking measured using bone and surface mounted markers*. Journal of Biomechanics, Vol. 40(15), 2007, p. 3412-3423.



NESTER, C. *Lessons from dynamic cadaver and invasive bone pin studies: do we know how the foot really moves during gait?* Journal of Foot and Ankle Research, Vol. 27, 2009 May, p. 2-18.

RATTANAPRASERT, U., SMITH, R., SULLIVAN, M., GILLEARD, W. *Three-dimensional kinematics of the forefoot, rearfoot, and leg without the function of tibialis posterior in comparison with normals during stance phase of walking.* Clinical Biomechanics (Bristol, Avon), Vol. 14(1), 1999 Jan, p. 14-23.

SAMSON, W., DOHIN, B., CHAVEROT, J.L., DESROCHES, G., DUMAS, R., CHEZE, L. *Scaling effect on dynamic gait parameters in young children.* In Revision

SAMSON, W., VAN HAMME, A., DUMAS, R., CHEZE, L. *Mechanical actions in a two-segment foot model: comparison of two methods,* Computer methods in Biomechanics and Biomedical Engineering. Accepted

SIMON, J., DOEDERLEIN, L., MC INTOSH, A.S., METAXIOTIS, D., BOCK, H.G., WOLF, S.I. *The Heidelberg foot measurement method: development, description and assessment.* Gait & Posture, Vol. 23(4), 2006 Jun, p. 411-424.

STEFANYSHYN, D.J., NIGG, B.M. *Mechanical energy contribution of the metatarsophalangeal joint to running and sprinting.* Journal of Biomechanics, Vol. 30(11-12), 1997 Nov-Dec, p. 1081-1085.

WANG, R., THUR, C.K., GUTIERREZ-FAREWIK, E.M., WRETENBERG, P., BROSTRÖM, E. *One year follow-up after operative ankle fractures: a prospective gait analysis study with a multi-segment foot model.* Gait & Posture, Vol. 31(2), 2010 Feb, p. 234-240.

WOODBURN, J., HELLIWELL, P.S., BARKER S. *Three-dimensional kinematics at the ankle joint complex in rheumatoid arthritis patients with painful valgus deformity of the rearfoot.* Rheumatology. Vol. 41(12), 2002, p. 1406-1412.

WU, G., CAVANAGH, P.R. *ISB recommendations for standardization in the reporting of kinematic data.* Journal of Biomechanics, Vol. 28(10), 1995 Oct, p. 1257-1261.

WU, G., SIEGLER, S., ALLARD, P., KIRTLEY, C., LEARDINI, A., ROSENBAUM, D., WHITTLE, M., D'LIMA, D.D., CRISTOFOLINI, L., WITTE, H., SCHMID, O., STOKES, I. *ISB recommendation on definitions of joint coordinate system of various joints for the reporting of human joint motion--part I: ankle, hip, and spine.* Journal of Biomechanics, Vol. 35(4), 2002 Apr, p. 543-548.

## Instructions Manual

Manuel d'instructions des Plateformes de forces Bertec®



## Other References

### Books

GUAY M., *Anatomie de l'appareil locomoteur*, PU Montreal, 2005

JENKINS, KEMNITZ, TORTORA, *Anatomy and Physiology From Science to Life*, John Wiley & Sons, Inc. 2007

KAPANDJI, I.A., *Physiologie articulaire 2. Membre inférieur*, Maloine, 1999

WITTENGURG, J., *Dynamics of Systems of Rigid Bodies*, B.G. Teubner Stuttgart, 1977

### Articles

RANKINE, L., LONG, J., CANSECO, K., HARRIS, G. *Multisegmental Foot Modeling: A Review. Critical Reviews in Biomedical Engineering*, Vol. 36(2-3), 2008, p. 127-181.



# Appendices

## A.1 Economical Cost

The economical cost of this study consists in the use of expensive scientific materials and the work of a trainee. The costs come from different sources: trainee salary, materials costs (and its depreciation), office costs and variables costs.

Firstly, **materials' depreciation cost** were calculated, dividing the unit cost by the number of hours of useful life, depreciation cost in euros/hour is obtained. The parameters and coefficients results are presented in Table A.1.1. util

	Unit Cost (€)	Utile Life (hours)	Depreciation cost (€/hour)
<b>Motion Analysis® System</b>	183 000	16 000	11,44
<b>Baropodometric Plate</b>	26 000	16 000	1,63
<b>Matlab® Software</b>	4 500	8 000	0,56
<b>Computer</b>	1 500	6 000	0,25
<b>Video Camera</b>	400	3 600	0,11

Table A.1.1 - Depreciation Costs

Secondly, an estimation of used hours for each material is estimated. It has been admitted:

		Use Time	Units	Subtotal (hours)	Total (hours)
<b>Motion Analysis System</b>	<b>Training</b>	5 h	1	5	40
	<b>Experimentation</b>	2 h / sub	10 sub	20	
	<b>Tracking</b>	1,5 h / sub	10 sub	15	
<b>Video Camera</b>		2 h /sub	10 sub	20	20
<b>Baropodometric Plate</b>	<b>Experimentation</b>	2 h /sub	10 sub	20	22,5
	<b>Data Exportation</b>	0,25 h / sub	10 sub	2,5	
<b>Salary trainee</b>		35 h / week	20 weeks	700	700
<b>Computer</b>		34 h / week	20 weeks	680	680
<b>Matlab® Software</b>		26 h / week	20 weeks	520	520

Table A.1.1 – Used Hours



The UPC ratio for project is considered, e.g. 12,7 % of the previous costs are considered as variables (electricity, heating and water consumed during the project)

Finally, the total cost, considering also consumables is detailed in Table A.1.3. The global cost of the project is **8 066,70 euros**.

		Unit Cost (€/hour)	Use (hours)	Cost (€)
<b>Motion Analysis</b>	<b>Motion Analysis<sup>®</sup> System</b>	11,44	40	457,60
	<b>Markers</b>	15 € / unit	38 units	570
	<b>Adhesive tape</b>	10 € / unit	3 units	30
<b>Computer</b>	<b>Computer</b>	0,25	680	170
	<b>Matlab<sup>®</sup></b>	0,56	520	291,20
<b>Others</b>	<b>Baropodometric Plate</b>	1,63	22,5	36,68
	<b>Video Camera</b>	0,11	20	2,20
<b>Trainee Salary</b>		8	700	5600
<b>Variable Costs (12,7 %)</b>				909,02
<b>Global Cost</b>				<b>80 66,70</b>

Table A.1.2 - Global Cost





## **A.2 Environmental and Social Impact**

The environmental impact of this study is quite moderated except in regards to the electronic waste of the materials used (computers, cameras, forceplates, baropodometric plate...) They form part of the Waste Electronic and Electrical Equipment (WEEE) and respond at the European Directive 2002/96/CE relative to their end of life treatment and possible.

There is obviously the impact of the use of energies as electricity and heating in the laboratory. In order not to do excessive waste, a cautious use of lights and heating must be applied.

However, it is more coherent to consider the social impact of the study. Indeed, the foot model developed here could be used for the study of pathologic clinical cases. Also, it could be useful for the shoe designers, for whom better knowledge of the foot movement evolution during gait could be efficient. Finally, the ankle orthoses and prostheses designers could be very interested in the use of such model.



### A.3 SCS Definition

The markers position allows the SCS definition as it is explained there. The information stored in Matlab® program for each segment are the coordinates of the unitary vector  $u$ , the unitary vector  $w$ , the distal point  $rD$  and of the proximal point  $rP$ .

The SCS definition is detailed for the right lower limb in the following.  
*Bold letter indicate a vector.*

#### Toes

- $rP2$ : Middle of HM1 and HM5
- $rD2$ :  $rP2$  plus **HM1 To**
- $u2$ : Normalized vector of (**HM1 HM5** x **HM1 To**)
- $w2$ : Normalized vector of (**To**  $rD2$ )

#### ForeFoot

- $rP3$ : Middle of BM1 and BM5
- $rD3$ :  $rP2$
- $u3$ : Normalized vector of (**BM1 HM5** x **BM5 HM1**)
- $w3$ : Normalized vector of (**HM1 HM5**)

#### MiddleFoot

- $rP4$ : Middle of Calca\_E and Calca\_I
- $rD4$ :  $rP3$
- $u4$ : Normalized vector of ( $rD4$   $rP4$  x ( $rP4$  Nav x  $rD4$   $rP4$ ))
- $w4$ : Normalized vector of (**BM1 BM5**)

#### HindFoot

- $rP5$ : Middle of Mal\_E and Mal\_I
- $rD5$ :  $rP4$
- $u5$ : Normalized vector of (**Calca\_E Nav**)
- $w5$ : Normalized vector of (**Calca\_E Calca\_I**)

#### Leg

- $rP6$ : Middle of Cond\_E and Cond\_I
- $rD6$ :  $rP5$
- $u6$ : Normalized vector of ( $rD6$   $rP6$  x  $rP6$  Fibula)
- $w6$ : Normalized vector of (**Mal\_I Mal\_E**)

#### Thigh

- $rP7$ : Hip Joint Center (calculated with circumduction trial)
- $rP7$ :  $rD6$
- $u7$ : Normalized vector of ( $rD7$   $rP7$  x  $w7$ )
- $w7$ : Normalized vector of (**Cond\_I Cond\_E**)

#### Pelvis

- $rP8$ : Lumbar Joint Center
- $rD8$ : Middle of the right and left hip joint center
- $u8$ : Normalized vector of ((**ASIS\_L ASIS\_R** x (**PSIS\_M ASIS\_M**))x(**ASIS\_L ASIS\_R**)
- $w8$ : Normalized vector of (**HJC\_L HJC\_R**)

where  $PSIS_M$  ( $ASIS_M$ ) is the middle of  $PSIS_R$  ( $ASIS_R$ ) and  $PSIS_L$  ( $ASIS_L$ )



### A. 4 BSIP

The coefficient table for men and women comes from Dumas et al. (2007). The coefficients are presented in the Table A.4.1 and A.4.2.

Scaling factors for :	Mass	Position of CoM			Inertia tensor					
	m (%)	X (%)	Y (%)	Z (%)	r <sub>xx</sub> (%)	r <sub>yy</sub> (%)	r <sub>zz</sub> (%)	r <sub>xy</sub> (%)	r <sub>xz</sub> (%)	r <sub>yz</sub> (%)
Entire Foot	1,2	43,6	-2,5	-0,7	11	25	25	9	6(i)	0
Leg	4,8	-4,8	-41	0,7	28	10	28	4(i)	2(i)	5
Thigh	12,3	-4,1	-42,9	3,3	29	15	30	7	2(i)	7(i)
Pelvis	14,2	2,8	-28	-0,6	101	106	95	25(i)	12(i)	8(i)

Table A.4.1 – BSIP Coefficients for Men

Scaling factors for :	Mass	Position of CoM			Inertia tensor					
	m (%)	X (%)	Y (%)	Z (%)	r <sub>xx</sub> (%)	r <sub>yy</sub> (%)	r <sub>zz</sub> (%)	r <sub>xy</sub> (%)	r <sub>xz</sub> (%)	r <sub>yz</sub> (%)
Entire Foot	1	44,3	4,4	-2,5	12	25	25	7(i)	5	3(i)
Leg	4,5	-4,8	-41	0,7	28	10	28	2	1	6
Thigh	14,6	-7,7	-37,7	0,9	31	19	32	7	2(i)	7(i)
Pelvis	14,6	-0,9	-23,2	0,2	91	100	79	34(i)	1(i)	1(i)

Table A.4.2 – BSIP Coefficients for Women



### A.5 Euler Angle Sequence Matrix

For the **ZXY mobile axes sequence**, the rotation matrix expressed in Wu and Cavanagh (2005) was used:

$${}^P_D R = \begin{bmatrix} \cos\alpha \cdot \cos\gamma - \sin\alpha \cdot \sin\beta \cdot \sin\gamma & -\sin\alpha \cdot \cos\beta & \cos\alpha \cdot \sin\gamma + \sin\alpha \cdot \sin\beta \cdot \cos\gamma \\ \sin\alpha \cdot \cos\gamma + \cos\alpha \cdot \sin\beta \cdot \sin\gamma & \cos\alpha \cdot \cos\beta & \sin\alpha \cdot \sin\gamma - \cos\alpha \cdot \sin\beta \cdot \cos\gamma \\ -\cos\beta \cdot \sin\gamma & \sin\beta & \cos\beta \cdot \cos\gamma \end{bmatrix} = [\delta_{ij}] \quad \text{Eq. A.5.1}$$

The 3 angles  $\alpha$  (Flexion),  $\beta$  (Abduction) and  $\gamma$  (Rotation) are derived by:

$$\alpha = \tan^{-1}\left(\frac{-\delta_{12}}{\delta_{22}}\right) \quad \beta = \sin^{-1}(\delta_{32}) \quad \gamma = \tan^{-1}\left(\frac{-\delta_{31}}{\delta_{33}}\right) \quad \text{Eq. A.5.2}$$

For the **ZYX mobile axes sequences**, the matrix expressed in Chèze et al. (2009) for the trapeziometacarpal joint was used:

$${}^P_D R = \begin{bmatrix} \cos\gamma \cdot \cos\alpha & \sin\beta \cdot \sin\gamma \cdot \cos\alpha - \cos\beta \cdot \sin\alpha & \cos\beta \cdot \sin\gamma \cdot \cos\alpha + \sin\beta \cdot \sin\alpha \\ \cos\gamma \cdot \sin\alpha & \sin\beta \cdot \sin\gamma \cdot \sin\alpha + \cos\beta \cdot \cos\alpha & \cos\beta \cdot \sin\gamma \cdot \sin\alpha - \sin\beta \cdot \cos\alpha \\ -\sin\gamma & \sin\beta \cdot \cos\gamma & \cos\beta \cdot \cos\gamma \end{bmatrix} = [\delta_{ij}] \quad \text{Eq. A.5.3}$$

The 3 angles  $\alpha$  (Flexion),  $\beta$  (Abduction) and  $\gamma$  (Rotation) are derived by :

$$\alpha = \tan^{-1}\left(\frac{\delta_{21}}{\delta_{11}}\right) \quad \beta = \tan^{-1}\left(\frac{\delta_{32}}{\delta_{33}}\right) \quad \gamma = \sin^{-1}(-\delta_{31}) \quad \text{Eq. A.5.4}$$



## A.6 Check List for Trials

For the trial capture, a check list has been created in order to not omit one detail that could cancel the trial done. An exemple of the check list used during the present study is presented there (in French).

### CHECK LIST

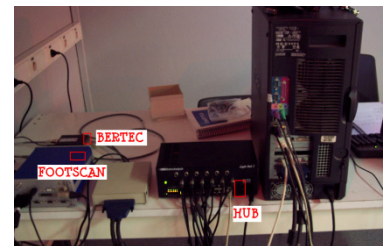
« Etude biomécanique de la marche de sujets sains »

#### PREPARATION MATERIEL

- ☐ 18 marqueurs 0.375" pour les pieds/ 20 marqueurs 0.75" pour le reste du corps → avec scotch physiologique
- ☐ Paire de ciseaux
- ☐ Appareil photo
- ☐ Mètre ruban
- ☐ Caméra + Pied Code porte (câble alimentation + câble pour synchronisation)

#### PREPARATION CAPTURE

- Vérifier le branchement de l'ensemble (Bertec®, Foot scan®, Motion Analysis®)
- Vérifier que la clé Motion est présente
- Allumer Bertec®, HUB, Caméras DV (mode démo =off), PC
- Dans C:\MANIPS\Angèle → nouveau dossier : *Sujet\_n*
- Copier projet11juillet.prj et forcepla.cal dans *Sujet\_n*
- Ouvrir Cortex (raccourci bureau)
- File → *Load Project* → C:\MANIPS\Marche\_Adulte\ *Sujet\_n* \ marche\_6cam.prj → open



#### SETUP

- Cliquer sur Connect To Cameras : 8 Eagle® Cameras + 1\_A-D Device National PCI → ok
- Paramètres par défaut sur ce projet : 100 Hz pour caméras & Bertec® ; voies 1 à 6 Bertec® 1, voies 7 à 12 Bertec® 2, voies 13 signal Trigger Footscan.

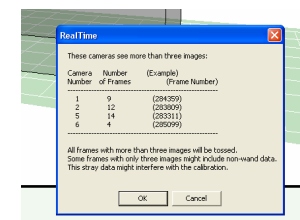
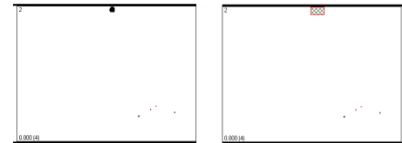
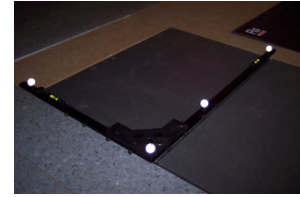


#### CALIBRATION

- Cliquer dans la zone du bas de l'écran : F2 (ou Dataview → 2D Display) : visualisation 2D des caméras
- All on : visualisation 2D des 8 caméras



- Enlever les masques éventuels du projet antérieur (Delete All masks)
- Cliquer sur Run
- Positionner Equerre
- Réglage du seuil et de la luminosité
- Régler le « Threshold » : environ 500 (jamais au-dessus de 700, cf recommandations constructeur). Luminosité = 100 en général. A régler selon l'image obtenue à l'écran.
- Vérifier que chaque caméra ne voit que les 4 points de l'équerre
- Si point « parasite » : clic molette maintenue sur la zone concernée → création d'un masque
- Settings / Calibration / Capture Volume (Capture Volume)
- Volume acquis par défaut : X : -500, 2500, Y: -700, 700, Z : 0, 1400
- Régler les caméras pour que leur champ de vision soit cohérent avec le volume d'acquisition – Attention à bien serrer les caméras sur leur pied (petite molette noire)
- Pour visualiser le champ des caméras : Show Field-Of-View
- Cliquer sur « Collect and Calibrate » (1<sup>er</sup>)
- Enlever l'équerre
- Vérifier qu'il n'y a plus de pas de point virtuel, sinon augmenter le seuil.
- Prendre la « Wand » (baguette de calibration)
- Cliquer sur « Collect and Calibrate » (2<sup>ème</sup>)
- Vérifier que pour chaque caméra *Number of Frames* soit faible (en dessous de 100 env., ms si optimisation ok, ok). Si une caméra n'est pas représentée, c'est que 100% des images vues par cette caméra contenait 3 points.
- Après dans Wand Processing Status, run again, jusqu'à stabilisation des valeurs (2-3 fois)
- Distance Avg 3D Residuals 0.5, wand length 500, et distance focale 18.
- Après avoir toutes les valeurs figées : Accept
- Save this as the "System Calibration"? → Yes → Ok
- ☐ Sauvegarder ensuite à nouveau, à partir du menu général : File → Save Project



## MOTION CAPTURE

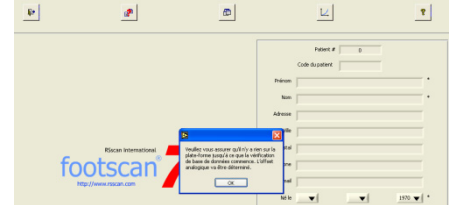
- ☐ Vérifier qu'il n'y a rien sur les PF de forces et Initialisation des PF de forces : Reset sur les boîtiers des PF.
- ☐ Output: **raw video**(img de chacune des cameras), **analog, tracked (ASCII)** , **ColorVideo**(.avi) → save project



- ☐ Name → **marche\_** (ou **static**, ou **circum** au début, en précisant si droite (d) ou gauche (g))

## FOOTSCAN

- ☐ Ouvrir **Footscan® 7** (raccourci bureau)
- ☐ A l'ouverture du logiciel, demande la longueur de la plateforme : choisir 1m
- ☐ Enlever tout élément sur la plateforme pour son initialisation → ok
- ☐ F2 (ou 3<sup>ème</sup> icône en haut) : base de données
- ☐ Ajouter patient → Nom/prénom/date de naissance → ok



## → ARRIVEE DU SUJET

## ENREGISTREMENT DES CARACTERISTIQUES DU SUJET

AQM	Nom	Prénom	Age	Taille (cm)	Pointure	Poids (kg)

## EQUIPEMENT DU SUJET

### « Petits marqueurs »

- ☐ Têtes du gros orteil
- ☐ Têtes du métatarse I
- ☐ Têtes du métatarse V
- ☐ Bases du métatarse I
- ☐ Bases du métatarse V
- ☐ Naviculaires
- ☐ Bords postérieurs du calcaneum
- ☐ Bords internes du calcaneum
- ☐ Bords externes du calcaneum

### « Gros marqueurs »

- ☐ Malléoles externes
- ☐ Malléoles internes
- ☐ Tubérosités tibiales antérieures
- ☐ Têtes des péronés
- ☐ Epicondyles fémoraux externes
- ☐ Epicondyles fémoraux internes
- ☐ Cuisses
- ☐ Grands trochanters
- ☐ Epines iliaques antéro-supérieures
- ☐ Epines iliaques postéro-supérieures

- Photos face et profil



CAPTURE

Dans Footscan

- ☐ Sélectionner le patient créé → Cliquer sur dynamique → Entrer Poids/pointure
- ☐ Appuyer sur l'icône d'acquisition dynamique (« bouton avec bonhomme »)

Retourner sur Cortex®

- ☐ Cocher l'enregistrement des fichiers .avi, .trc, .vc, .anb
- ☐ Record
- ☐ Passage du sujet
- ☐ A la fin de l'acquisition, retourner sur RsScan® → F7 (ou save) en appelant le fichier « \_n » (où est le numéro de passage du sujet (le même que sur Cortex®). Bien réappuyer sur le « bonhomme bleu » pour faire une nouvelle acquisition de RsScan®)
- ☐ Réaliser une acquisition statique sur le tapis de pression pour avoir une référence  
/!\ A ce que tous les marqueurs (38) soient bien dans le champ de vision des caméras.
- ☐ Réaliser une acquisition de circumduction.

VERIFICATION FINALE

On doit avoir des acquisitions de type:

- ☐ Marche conventionnelle
- ☐ Une statique
- ☐ 2circumductions

Enlever les marqueurs / Remerciements

FIN DE MANIPULATION

- ☐ Eteindre Bertec®
- ☐ Eteindre Hub
- ☐ Eteindre RSscan®
- ☐ Eteindre Caméras DV
- ☐ Eteindre PC

EXPORTATION DES DONNEES

- RsScan® : Sélection de chacun des essais,
- Export de la BD (Enregistrement des fichiers sources .fpm)
- Export, sélection du roll-off (Dynamic Roll Off) et de la pression max (Dynamic Maximum Image)
- Cortex® : Récupérer le dossier correspondant au sujet créé par Cortex®.





## A.7 Accepted Abstract

# Mechanical actions in a two-segment foot model: comparison of two methods

W. SAMSON<sup>†‡\*</sup>, A. VAN HAMME<sup>‡</sup>, R. DUMAS<sup>‡</sup> and L. CHEZE<sup>‡</sup>

<sup>†</sup> CTC - Comité Professionnel de Développement Economique Cuir Chaussure Maroquinerie,  
4 rue Hermann Frenkel - 69 367 LYON Cedex 7, France

<sup>‡</sup> Université de Lyon, Lyon F-69003, France  
Université Lyon 1, F-69003, France

Institut National de Recherche sur les Transports et leur Sécurité, Bron F-69675, France  
Laboratoire de Biomécanique et Mécanique des Chocs - UMR\_T 9406, UFR Mécanique,  
Villeurbanne F-69622, France

\*Corresponding author. Email: wsamson@ctcgroupe.com

*Keywords:* foot; multi-segment model; dynamic; plantar pressure

## 1 Introduction

Modeling the foot as one rigid segment is inadequate for clinical decisions making for patients with foot impairments [1]. Several works have developed multi-segment model in order to evaluate the foot posture. Kinematic validation has already been realized about models with more than three segments [2,3]. In dynamic, due to the methodology problem (i.e. distribution of force plate data on each foot segment), few studies have explored the inter-segment mechanical actions (i.e. joint forces and moments). MacWilliams et al. [1] defined these actions distributing the force plate data under each foot segment from a plantar pressure plate. The authors hypothesize that shear forces and twisting moments are distributed among each segment in proportion to the normal force. However, the effects of this hypothesis are not demonstrated. Then, the aim of this study is to compare the values of mechanical actions under foot segments calculated from different methods.

## 2 Methods

Ten subjects were measured during gait trial at self-selected speed. Six retro-reflective markers were fixed on anatomical landmarks of right foot: medial, lateral and posterior calcaneum, medial and lateral metatarsus, and toe I. Gait trials were

measured for each subject using a Motion Analysis® system with eight Eagle® cameras (Santa Rosa, USA), one Bertec® force plate (Colombus, USA) and one Footscan® plantar pressure plate (Olen, Belgium) synchronized to a sampling frequency of 100 Hz. Stance phases were recorded during two trials: (i) with two force plates (condition **a**); (ii) one plantar pressure plate (condition **b**) and one force plate (condition **c**) (Figure 1a-c).

From the condition **a**, forefoot ( $\vec{F}_{ff}$ ,  $\vec{M}_{ff}$ ) and rearfoot ( $\vec{F}_{rf}$ ,  $\vec{M}_{rf}$ ) mechanical actions were processed on each center of pressure ( $O_{ff}$ ,  $O_{rf}$ ). The equation of the straight line ( $D$ ) cutting the foot in two parts (i.e. forefoot and rearfoot) was processed using the foot landmark.

From the condition **b**, the maximum plantar pressure of each pixel defined the foot area. The foot was segmented following the straight line ( $D$ ), previously defined. After that, the pressure barycenters of the two areas defined the coordinates  $O_{ff}$  and  $O_{rf}$ , expressed as function of foot area proportions. The  $\vec{F}_{y_{ff}}$  and  $\vec{F}_{y_{rf}}$  were the sum of vertical forces acting on forefoot and rearfoot areas, respectively.

From the condition **c**, mechanical actions ( $\vec{F}_f$ ,  $\vec{M}_f$ ) were processed on the center of pressure ( $O_f$ ).



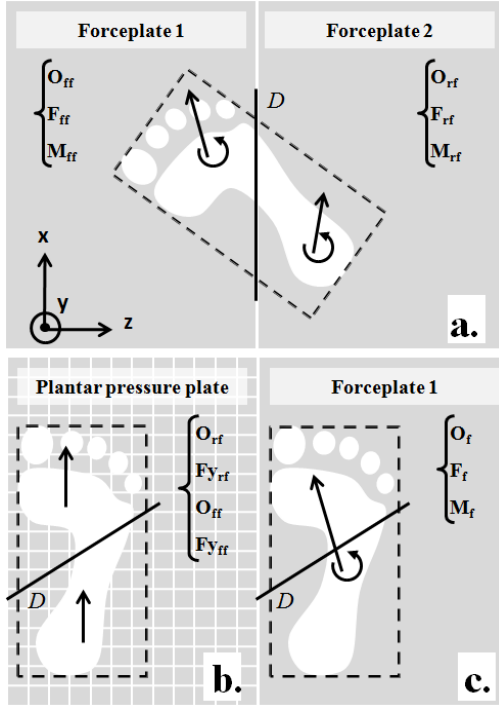


Figure 4: foot contact on two forceplates (a), one plantar pressure plate (b) and one forceplate (c)

Then, after the cutting of foot following the straight line (D) (Figure 1c), two approaches were considered for calculating rearfoot and forefoot mechanical actions in the condition c:

(i)  $\vec{M}_f$  can be expressed as follow [1]:

$$\vec{M}_f = \vec{M}_{ff} + \vec{O}_f \vec{O}_{ff} \wedge \vec{F}_{ff} + \vec{M}_{rf} + \vec{O}_f \vec{O}_{rf} \wedge \vec{F}_{rf} \quad (1)$$

The hypothesis was made that the shear forces ( $\vec{F}_{x_{ff}}, \vec{F}_{x_{rf}}, \vec{F}_{z_{ff}}$  and  $\vec{F}_{z_{rf}}$ ) and the free torques ( $\vec{M}_{y_{ff}}$  and  $\vec{M}_{y_{rf}}$ ) were distributed as function of foot vertical force ( $\vec{F}_{y_f}$ ) and foot free torque ( $\vec{M}_{y_f}$ ) respectively; therefore:

$$\begin{cases} \begin{cases} \vec{F}_{ff} \\ \vec{M}_{y_{ff}} \end{cases} = k_1 \begin{cases} \vec{F}_f \\ \vec{M}_{y_f} \end{cases} \\ \begin{cases} \vec{F}_{rf} \\ \vec{M}_{y_{rf}} \end{cases} = (1 - k_1) \begin{cases} \vec{F}_f \\ \vec{M}_{y_f} \end{cases} \end{cases} \quad (2)$$

with  $k_1$ , the proportion of foot vertical force used by forefoot in the condition b.

(ii) The alternative method is based on the Coulomb's laws, stating that the shear forces and

the free torque could be expressed as function of vertical force :

$$\begin{cases} \|\vec{F}_{xz_f}\| = k_2 \|\vec{F}_{y_f}\| \\ \|\vec{M}_{y_f}\| = k_3 \|\vec{F}_{y_f}\| \end{cases} \quad (3)$$

with  $k_2$  and  $k_3$ , the friction and resistance coefficients, respectively. Then, the hypothesis was made that the proportion of  $\|\vec{F}_{xz_f}\|$  on axis x and z, is the same for entire foot, forefoot and rearfoot.

Finally, the mechanical actions measured in the condition a were compared with the mechanical actions calculated from the two previous approaches.

### 3 Results and Discussion

Both approaches showed differences between the values of mechanical actions under the forefoot and the rearfoot comparing to these mechanical actions in the condition a. As a consequence of these differences, even if the differences were small, the inter-segment mechanical actions between forefoot and rearfoot, computed from both results, were not the same in comparison with the condition a.

### 4 Conclusions

The study showed that the hypotheses on which the distribution of the shear forces and free torques is based has an effect on inter-segment mechanical actions. Future works will combine foot kinematic and plantar pressure measurement in order to reduce the effects of foot area's definition and intra-individual variability of gait.

1/

### References

- [1] MacWilliams B.A., Cowley M., and Nicholson D.E., Foot kinematics and kinetics during adolescent gait. *Gait and Posture* 2003, 17,214-224.
- [2] Leardini A., Benedetti M.G., Berti L., Bettinelli D., Natio R., and Giannini S., Rear-foot, mid-foot and fore-foot motion during the stance phase of gait. *Gait & Posture* 2007, 25, 453-462.
- [3] Lundgren P., Nester C., Liu A., Arndt A., Jones R., Stacoff A., Wolf P., and Lundberg A. Invasive in vivo measurement of rear-, mid- and forefoot motion during walking. *Gait & Posture* 2008, 28, 93-100.

